

New Detectors Ideas: Work in Progress

Giovanni Carugno
INFN & UNIPD

- A short list of theoretical motivations
- New Possible Low Energy Active Detectors: Ideas and Facts
- Single Spin Flip Electron Detection (**Cosmological Axions**)
- Low Temperature Single Electron Detection (**Light WIMPS & Neutrinos**)
- Single Atomic Excitation Detection through Laser Probe
- Perspectives and Conclusions

Che tu sappia prendere la parte di mondo che ti appartiene

Piero Dal Piaz

Low energy @ Weak cross section scale:

Tentative List

- Dark matter : Cosmological Axion Detection & Light WIMPS
- Two neutrinos emissions from Atoms
- Neutrino scattering via Coherent Z_0 channel
- Neutrino Torque on Spin
- Laser Induced Electron Capture Enhancement
- Nuclear and Electron Spin driven laser precession
- Artificial Atoms for T violation experiment

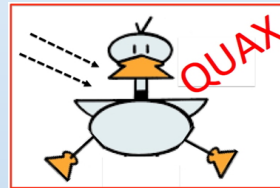
Low Energy Threshold Detectors: *from 50 μeV to eV*

- A) Strong coupling regime between Electron Spin and E.M. Cavity { **QUAX** }
From Field Amplitude to Energy measurement
Single Photon Microwave Detector
- B) Infrared Quantum Counter (Bloembergen Idea) { **AXIOMA-g** }
Zeeman Magnetic Type M1 Transition Detection
Rare Earth or Transition Metals doped crystal
Fluorescence Photon Detection
- C) Matrix Isolation Spectroscopy { **AXIOMA-e** }
Solid Neon/Methane/Para-Hydrogen Matrix Doped Crystals
(host atoms retain almost the structure of free atoms)
Single Electron Detection

Searching for Galactic Axions

QUAX Status

QUest for AXions



Giovanni Carugno

on behalf of the QUAX Collaboration



Overview

- Axion-electron coupling: DFSZ models (in KSVZ models $1/\alpha$ suppression)
- Detection principle: electron spin resonance (ESR)
- Experimental challenges: current R&D @ INFN
- Current sensitivity of the QUAX prototype
- Axion-Photon coupling sensitivity with QUAX set up

Interaction of DFSZ axion and electron spin

- The interaction of the DFSZ axion with a spin ½ particle

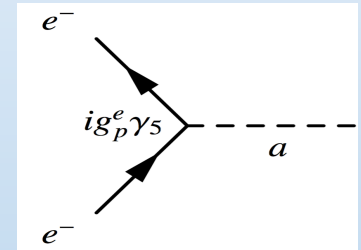
$$\mathcal{L}_{a,\text{matter}} = f_a^{-1} g_{aij} \bar{\Psi}_i \gamma^\mu \gamma^5 \Psi_j \partial_\mu a$$

$$g_p \cong \frac{m_e}{3f_a} \cos^2 \beta$$

$$g_p \approx 3 \times 10^{-11} \left(\frac{m_a}{1 \text{ eV}} \right)$$

- DFSZ axion coupling with non relativistic ($v/c \ll 1$) electron: equation of motion reduces to the Schroedinger equation

$$i\hbar \frac{\partial \varphi}{\partial t} = \left[-\frac{\hbar^2}{2m} \nabla^2 - \frac{g_p \hbar}{2m} \sigma \cdot \nabla a \right] \varphi$$



- Cold Dark Matter of the Universe may consists of axions and they can be searched for

The interaction term has the form of a **spin - magnetic field interaction** with $\vec{\nabla} a$ role of an **oscillating effective magnetic field**

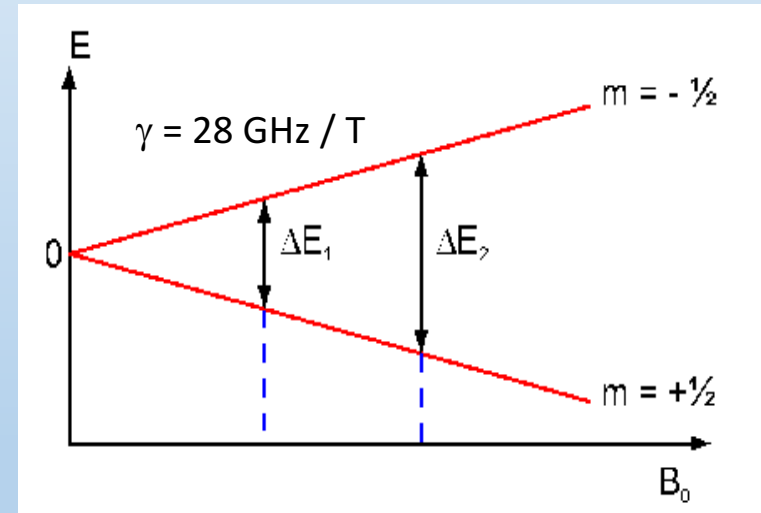
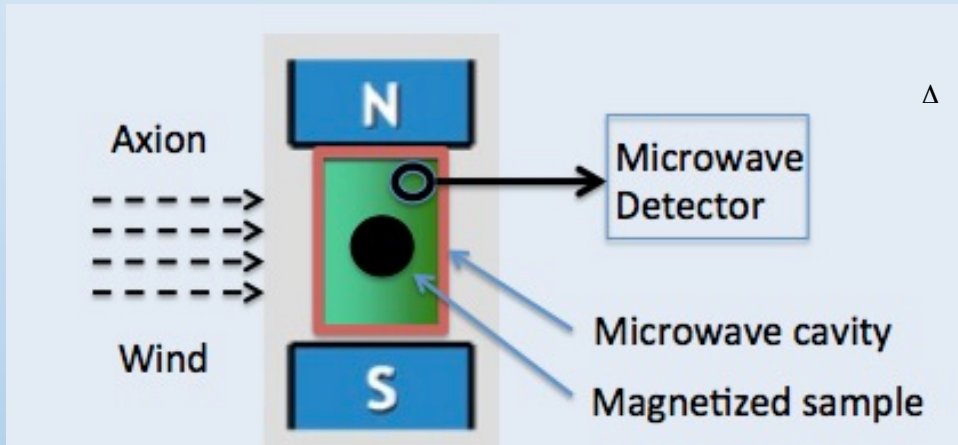
$$\mathbf{H}_{\text{int}} = -2\mu_B \vec{\sigma} \cdot \left[\frac{g_p}{2e} \vec{\nabla} a \right]$$

$$\mathbf{B}_a = \frac{g_p}{2e} \vec{\nabla} a$$

- **Frequency** of the effective magnetic field proportional to **axion energy**
- **Amplitude** of the effective magnetic field proportional to **axion density**

The Axion Wind

- Due to the motion of the solar system in the galaxy, the axion DM cloud acts as an effective RF magnetic field on electron spin
- RF field excites magnetic transition in a **magnetized sample** (Larmor frequency) with a static magnetic field B_0 and can produce a detectable signal
- The interaction with axion field produces a variation of magnetization which is in principle measurable



Idea is not new and comes from **several works**:

- L.M. Krauss, J. Moody, F. Wilczek, D.E. Morris, "Spin coupled axion detections", HUTP-85/A006 (1985)
- R. Barbieri, M. Cerdonio, G. Fiorentini, S. Vitale, Phys. Lett. B 226, 357 (1989)
- F. Caspers, Y. Semertzidis, "Ferri-magnetic resonance, magnetostatic waves and open resonators for axion detection", Workshop on Cosmic Axions, World Scientific Pub. Co., Singapore, p. 173 (1990)
- A.I. Kakhizde, I. V. Kolokolov, Sov. Phys. JETP 72 598 (1991)

The Axion effective magnetic field

- R. Barbieri et al., *Searching for galactic axions through magnetized media: The QUAX proposal* [Phys. Dark Univ. **15**, 135 - 141 (2017)]

The effective magnetic field associated with the axion wind

$$B_a = \frac{g_p}{2e} \left(\frac{n_a h}{m_a c} \right)^{1/2} m_a v_E$$

n_a – axion density $\sim 0.4 \text{ GeV/cm}^3$
 v_E – Earth velocity $\sim 220 \text{ km/s}$
 axion velocity dispersion $\sim 270 \text{ km/s}$

Using from standard model of Galactic Halo:

$$B_a = 2.0 \cdot 10^{-22} \left(\frac{m_a}{200 \mu\text{eV}} \right) \text{ T,}$$

$$\frac{\omega_a}{2\pi} = 48 \left(\frac{m_a}{200 \mu\text{eV}} \right) \text{ GHz,}$$

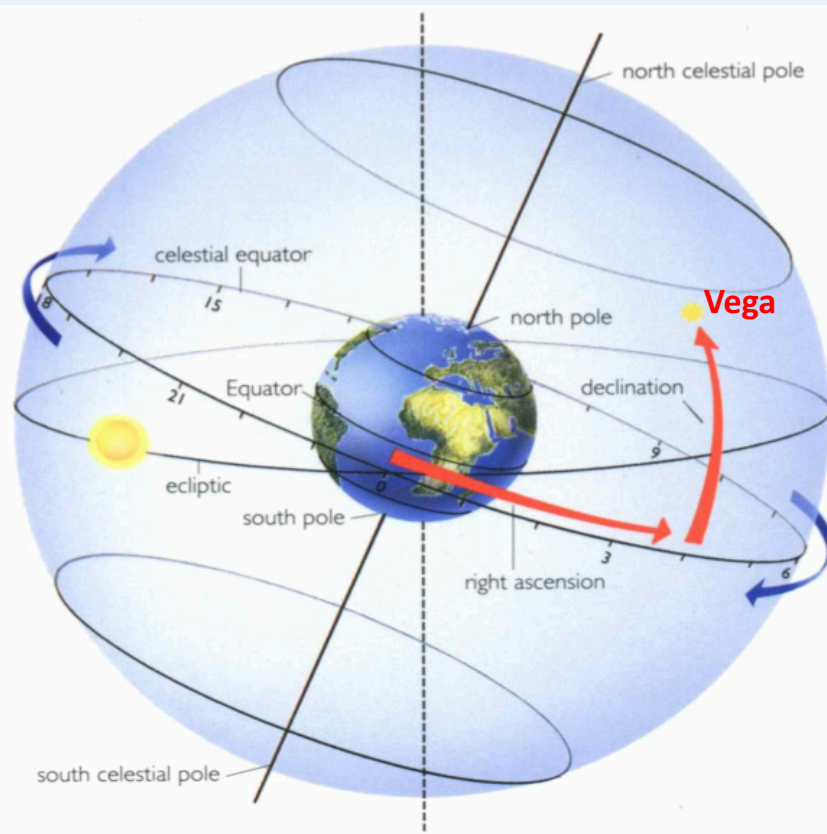
$$\tau_{\nabla a} \simeq 0.68 \tau_a = 17 \left(\frac{200 \mu\text{eV}}{m_a} \right) \left(\frac{Q_a}{1.9 \times 10^6} \right) \mu\text{s;}$$

Coherence time

$$\lambda_{\nabla a} \simeq 0.74 \lambda_a = 5.1 \left(\frac{200 \mu\text{eV}}{m_a} \right) \text{ m,}$$

Correlation length

Polarized Matter: directional DM search



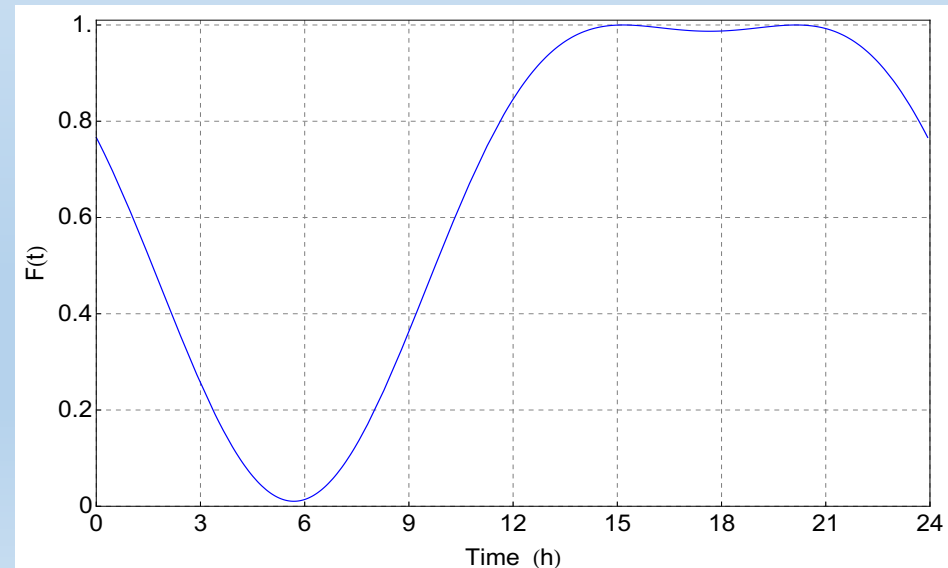
Due to Earth rotation, the direction of the static magnetic field B_0 changes with respect to the direction of the axion wind (Vega in Cygnus)

e.g. QUAX located @Legnaro (PD)

B_0 in the local horizontal plane and oriented N-S (the local meridian)

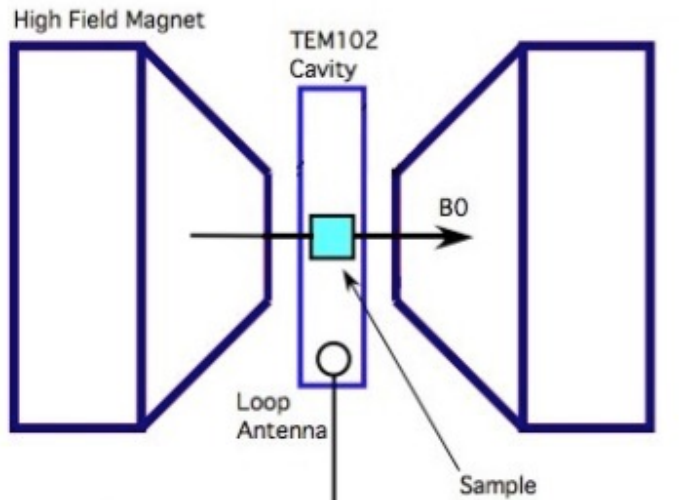
Strong modulation (up to 100%)!
Not due to seasonal or Earth rotation Doppler effect (few %) but to relative direction change of magnetic field respect to axion wind

QUAX Pattern



Detection strategy: Electron Spin Resonance

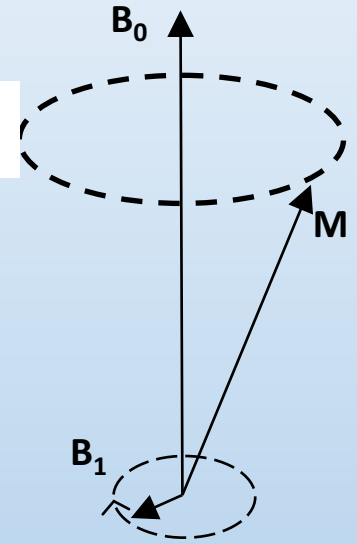
Electron spin resonance (ESR) arises when energy levels of a quantized system of electronic moments are **Zeeman split** (the **magnetic system** is placed in a uniform magnetic field B_0) and the system absorbs/emits EM radiation (in the microwave range) at the **Larmor frequency** ν_L of the **ferromagnetic resonance**.



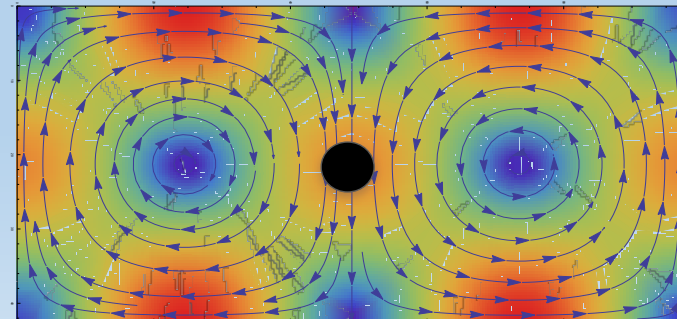
$$B = \begin{pmatrix} B_1 \cos(\omega t) \\ B_1 \sin(\omega t) \\ B_0 \end{pmatrix} \quad \nu_L = \gamma B_0$$

$\gamma = 28 \text{ GHz / T}$

1.7 T \rightarrow $\nu_L = 48 \text{ GHz}$



TEM102 Resonant Cavity
 B_0 along z axis (normal to the figure)



- An experimental geometry with **crossed field** is needed:
- B_0 along the z direction, defines the Larmor resonance
 - RF field B_1 in the x-y plane excites the Magnetization modes

The system macroscopic dynamics is given by **Bloch equations** which describe the evolution of **each component** of the magnetization vector \mathbf{M} . **No radiation damping in a resonant cavity and in strong coupling regime of Kittel/cavity modes.**

Axion driving of magnetization

The axion wind mimics the transverse rf magnetic field inducing a **time dependent magnetization of the uniform or Kittel mode** of the magnetized sample

$$M_a(t) = \gamma \mu_B B_a n_S \tau_{\min} \cos(\omega_a t),$$

at resonance

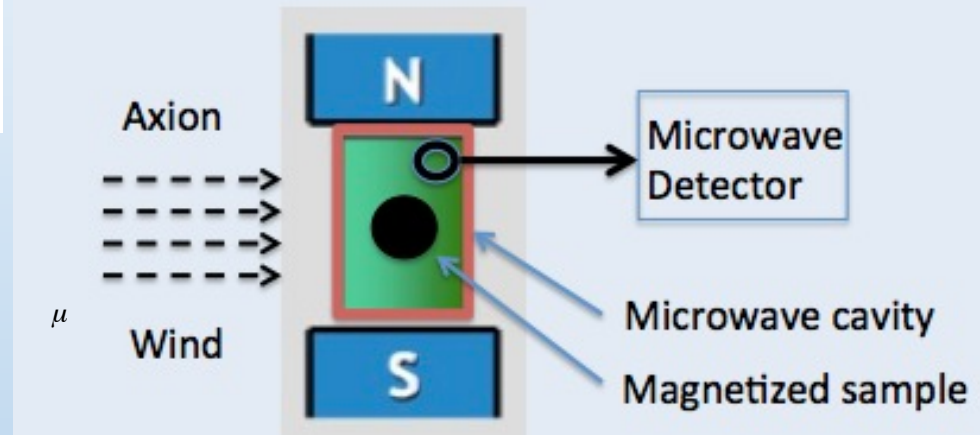
τ_{\min} is the shortest coherence time among:

- axion wind coherence τ_{∇_a}
- magnetic material relaxation time τ_2
- radiation damping τ_r

n_S – material spin density

μ_B – Bohr magneton

μ



A volume V_s of magnetized material will absorb energy from B_a at a rate

$$P_{\text{in}} = \mu_0 \mathbf{H} \cdot \frac{d\mathbf{M}}{dt} = B_a \frac{dM_a}{dt} V_s = \gamma \mu_B n_S \omega_a B_a^2 \tau_{\min} V_s$$

this power will excite magnetization/cavity modes and could be possibly detected

Anticipated signal strength

Expected signal as a function of relevant experimental parameters

Working @ $m_a = 200 \mu\text{eV} \rightarrow 48 \text{ GHz}$

**Larmor frequency tuning
by magnetizing field
 $B_0 = 1.7 \text{ T} \Rightarrow 48 \text{ GHz}$**

$$P_{\text{out}} = \frac{P_{\text{in}}}{2} = 3.8 \times 10^{-26} \left(\frac{m_a}{200 \mu\text{eV}} \right)^3 \left(\frac{V_s}{100 \text{ cm}^3} \right) \left(\frac{n_S}{2 \cdot 10^{28} / \text{m}^3} \right) \left(\frac{\tau_{\text{min}}}{2 \mu\text{s}} \right) \text{ W}$$

Such a low power level is out of reach of linear amplifiers



**Single photon
microwave detection**

To be developed

See discussion in *S.K. Lamoreaux et al., Phys. Rev. D 88 (2013) 035020*.

The corresponding
signal photon rate

$$R_a = \frac{P_{\text{out}}}{\hbar\omega_a} = 1.2 \times 10^{-3} \text{ Hz}$$

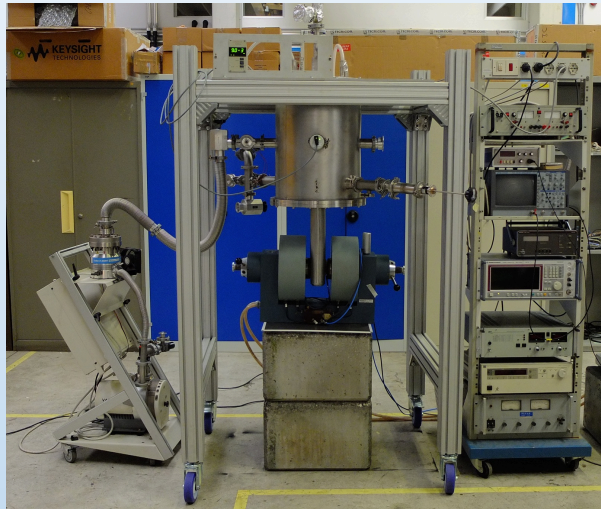
**this rate establishes the required dark count
rate of the photon counter**

QUAX experimental challenges

- **Magnetized material**
 - Spin density $2 \times 10^{28} / \text{m}^3$
 - Ferromagnetic linewidth $\sim 150 \text{ kHz}$ (i.e. $\tau_2 \sim \mu\text{s}$)
 - Total volume $\sim 100 \text{ cm}^3$
- **Microwave cavity**
 - Q factor $\gtrsim 10^6$
 - To be operated in a few Tesla static magnetic field
 - Must house a 100 cm^3 magnetic sample (use replica?)
- **Magnetizing field**
 - Up to 2 T magnetic source
 - High uniformity and high stability – at the ppm level
- **Microwave receiver**
 - Single photon counter with a dark count rate $\lesssim 10^{-3} \text{ Hz}$
- **Complete apparatus**
 - Working temperature around 100 mK
 - Noise dominated by thermodynamic fluctuations
 - Frequency tunability (to search for different axion masses)

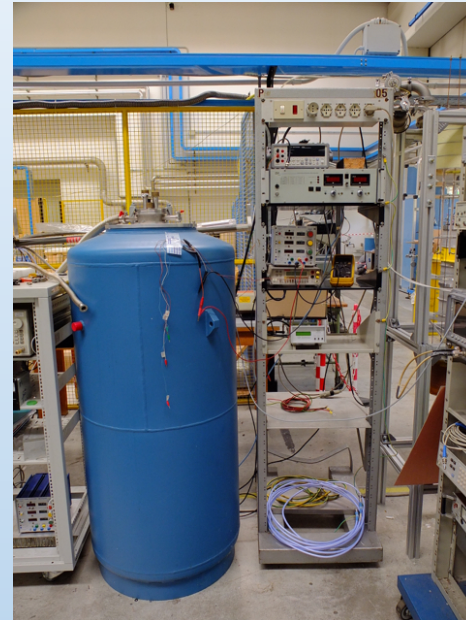
Work in progress

We are working on almost all these points to address the feasibility of the experiment



Cryogenic system #1 in Legnaro

External magnetic source



Cryogenic system #2 in Legnaro
Superconducting magnet



Cryogenic system in Frascati Superconducting magnet



All present systems works with LHe
A dilution refrigerator is on the way

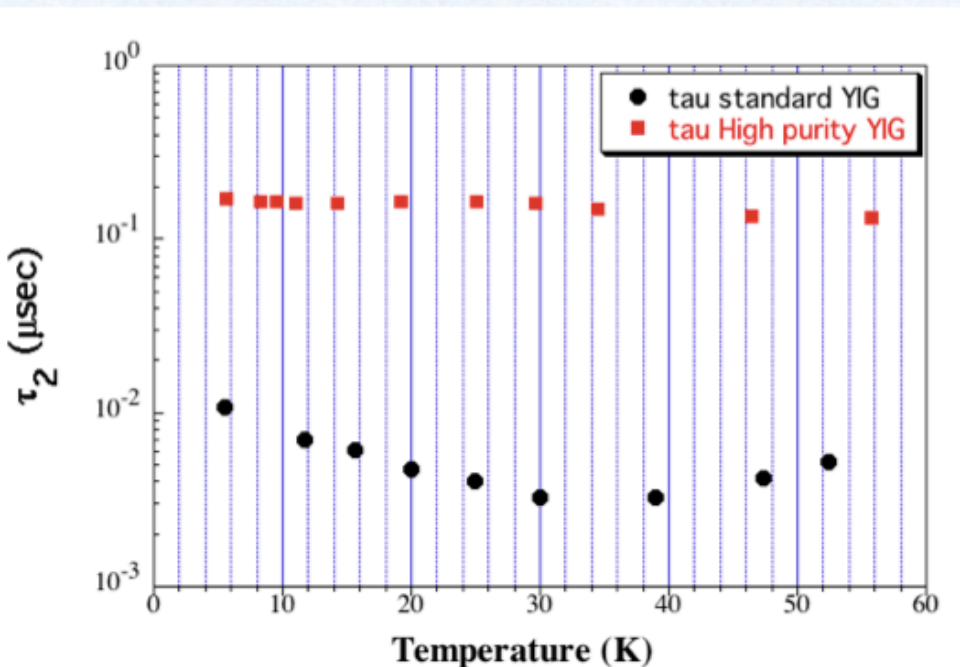
During R&D we are working in the 10 – 15 GHz range

Magnetic Material

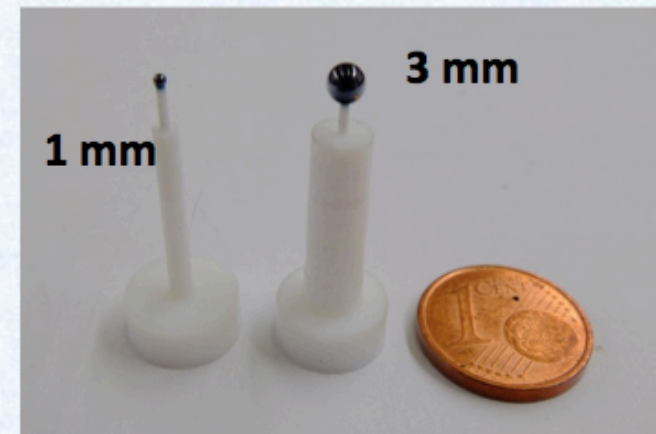
Material	Spin density	M0	τ_1	τ_2	Size
YIG	2.1×10^{28} [1/m ³]	1.4×10^5 A/m	$0.16 \mu\text{s}$	$0.16 \mu\text{s}$	Spheres 1 mm, 2 mm and 3 mm diameter
All values at room temperature					

YIG – Yttrium Iron Garnet is a ferrimagnetic synthetic garnet with chemical composition $\text{Y}_3\text{Fe}_5\text{O}_{12}$.

Its **ferromagnetic linewidth** ($= 1 / 2 \pi \tau_2$) depends on temperature, **sample purity** and geometry (highly polished spheres)



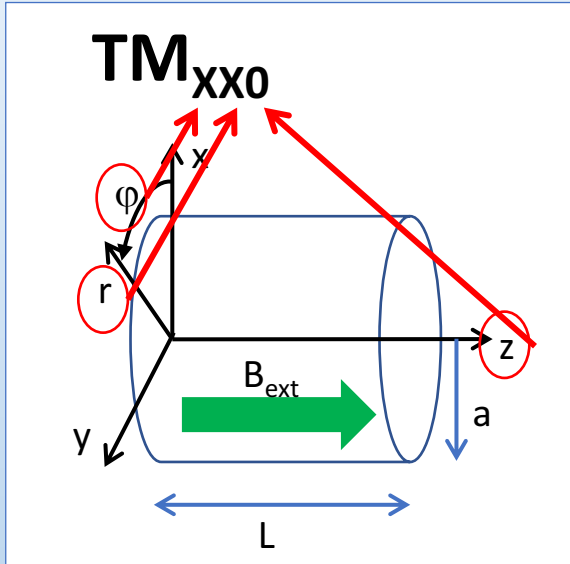
Typical application: rf filters and synth



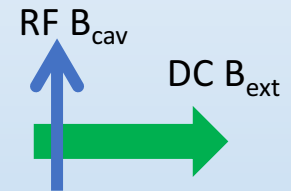
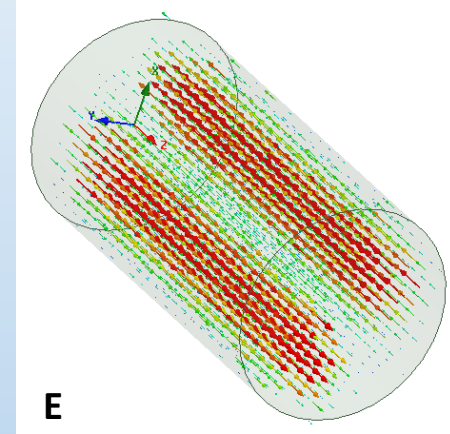
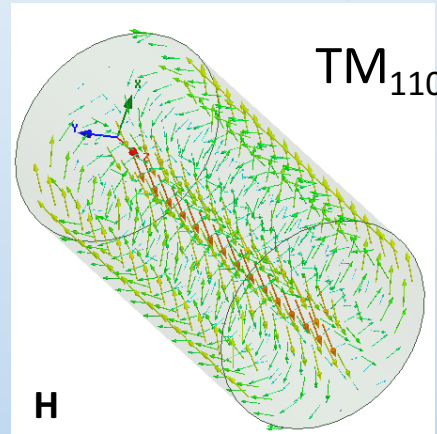
High purity YIG:
rare earth content below **1 ppm**

Microwave Cavity: Geometry

Basic geometry: **cylindrical cavity** working in the **TM_{xx0}** mode



- Simple design
- RF field uniform along the longitudinal coordinate
- Resonance frequency fixed by the radius of the cell



To increase the volume of the cavity (for YIG or other material insertion) we have to increase the **cavity length**. This does not change the resonance frequency.



This **increases the number of nearest modes** (hybridization can couple different modes?)

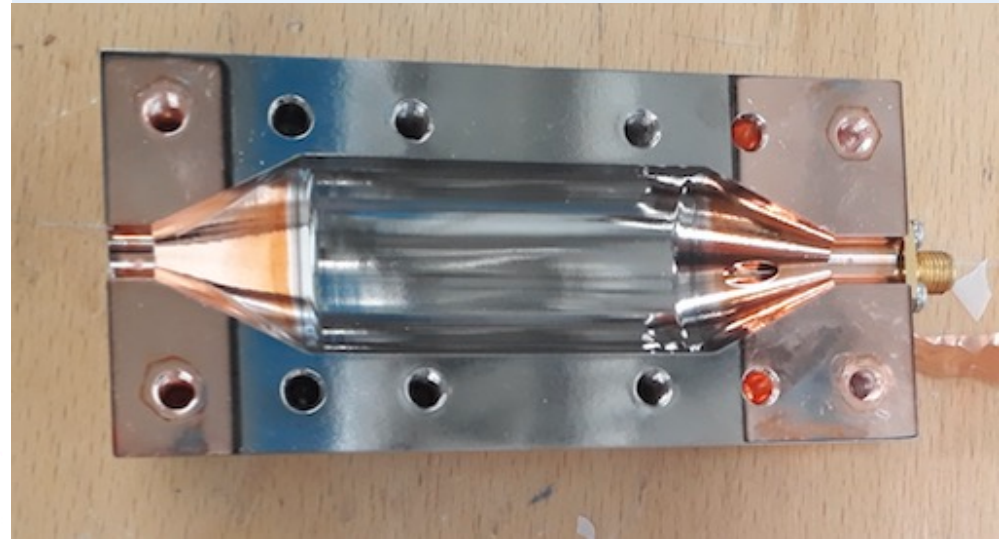
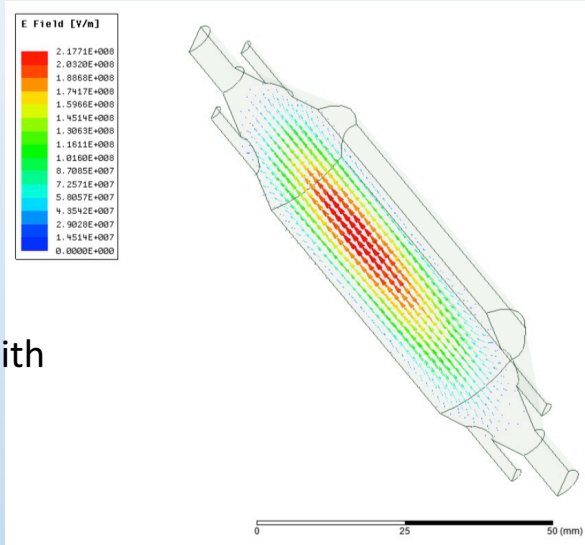
Cylindrical geometry produces mode degeneracy for the chosen mode



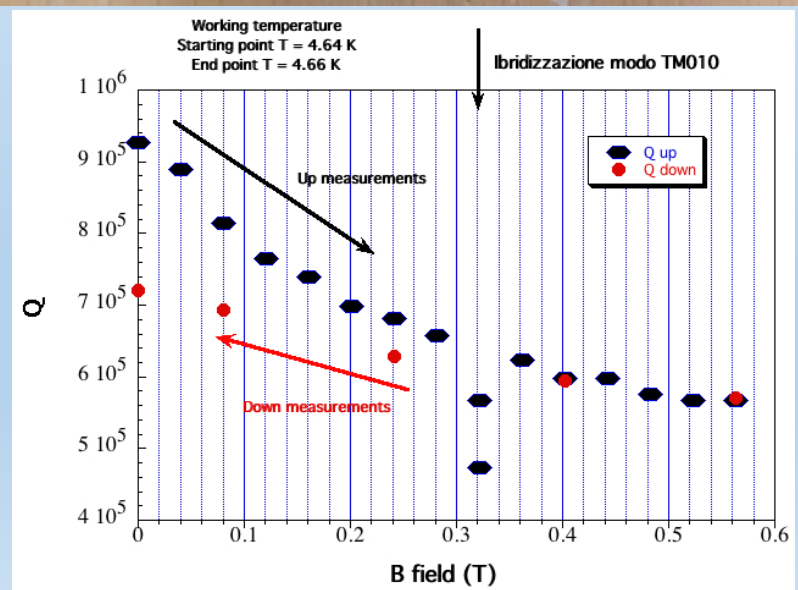
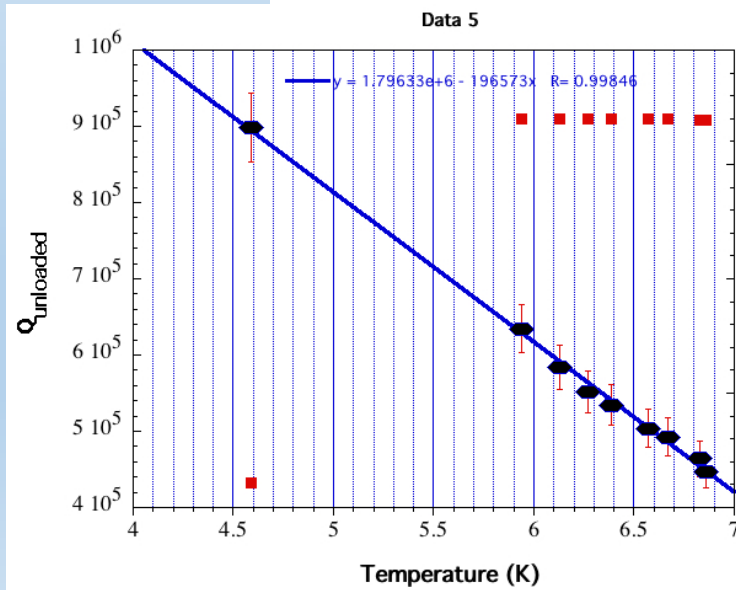
Solved by employing structure cuts

High Q cavity in external field

TM010
MODE



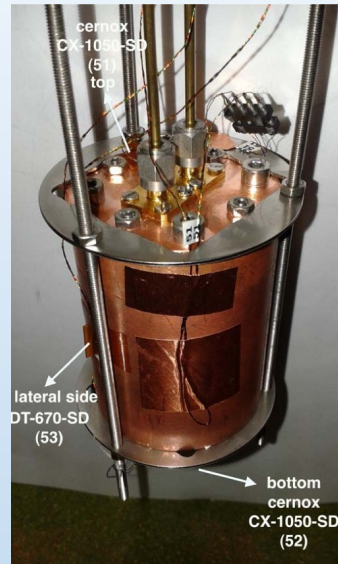
Cylindrical cavity with
conical endcaps



Microwave Cavity: Measurements

Cavity design for 14 GHz resonance frequency

Diameter = 26.1 mm
Length = 50.3 mm



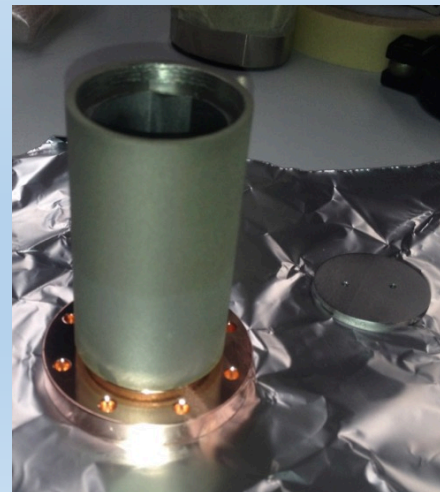
Copper cavity

Courtesy S. Gallo

$T = 300\text{ K}$
 $f_c = 13.999\text{ GHz}$
 $Q_0 = 1.8 \cdot 10^4$

$T = 4.2\text{ K}$
 $f_c = 14.045\text{ GHz}$
 $Q_0 = 5.4 \cdot 10^4$

Niobium cavity



$T = 300\text{ K}$
 $f_c = 13.957\text{ GHz}$
 $Q_0 = 4.2 \cdot 10^3$

$T = 4.2\text{ K}$
 $f_c = 13.934\text{ GHz}$
 $Q_0 = 6.9 \cdot 10^5$

Short Niobium cavity **with cut** along the side wall



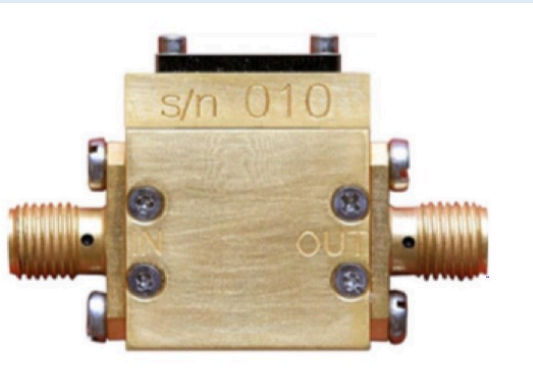
$T = 300\text{ K}$
 $f_c = 13.964\text{ GHz}$
 $Q_0 = 5.0 \cdot 10^3$

$T = 4.2\text{ K}$
 $f_c = 13.960\text{ GHz}$
 $Q_0 = 5.0 \cdot 10^5$

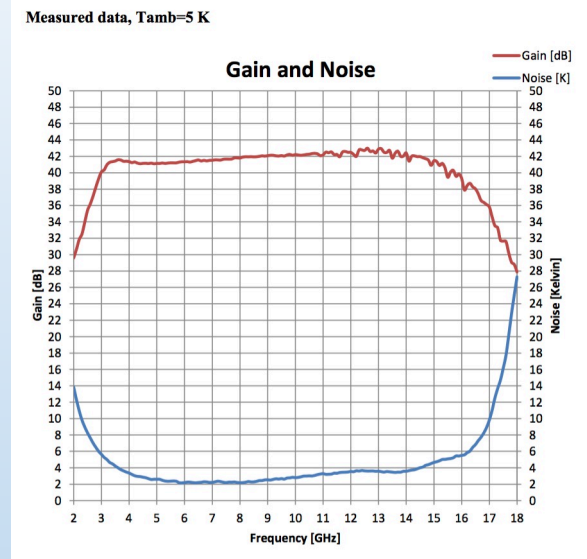
- Measurements of the effect of the external magnetic field are going on
- We have to check the inside magnetic field

Microwave Receivers: HEMT, JPA, SPD

- All our tests for the moment are conducted with a **low noise linear amplifier**



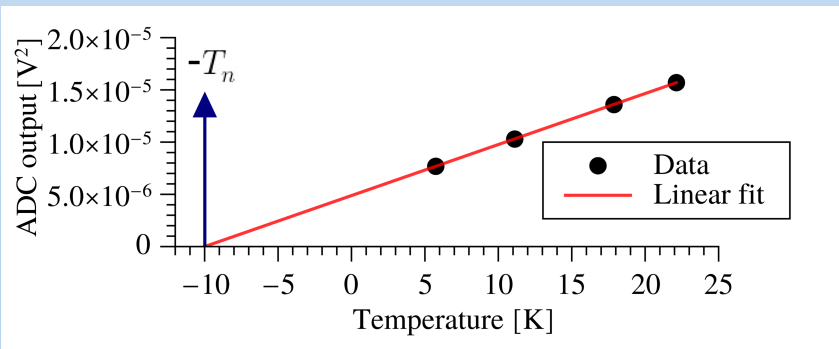
HEMT
High Electron
Mobility
Transistor



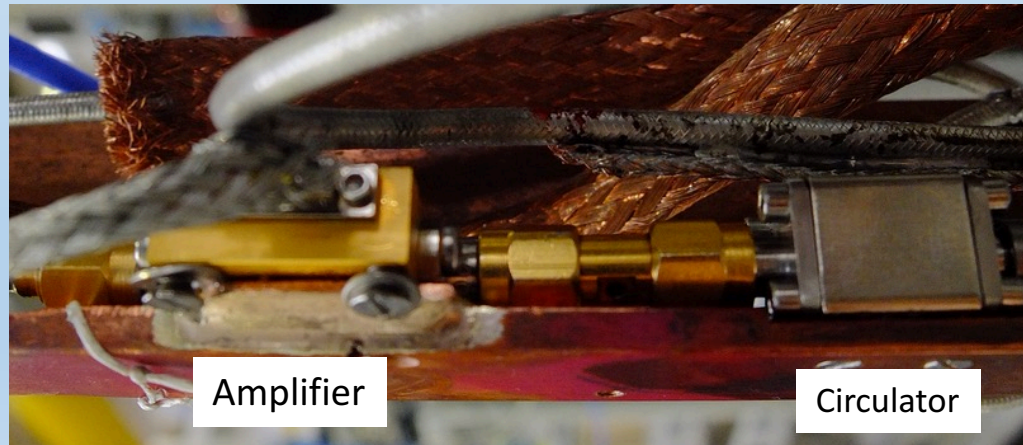
@ 14 GHz
@ 5 K

$T_n = 4$ K

Amplifier noise Temperature @ 5 K



Mounted amplifier has a T_n about two times bigger than specification



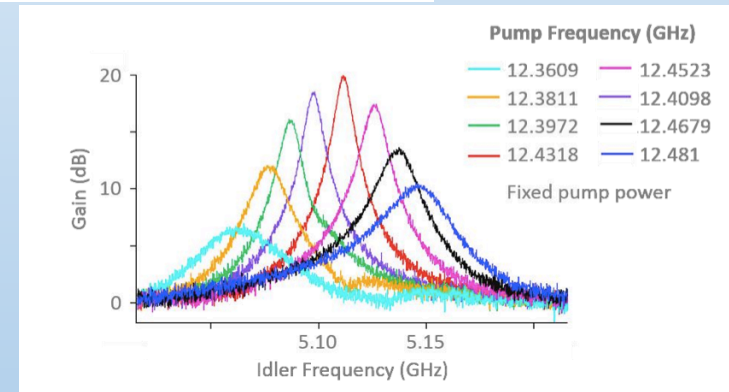
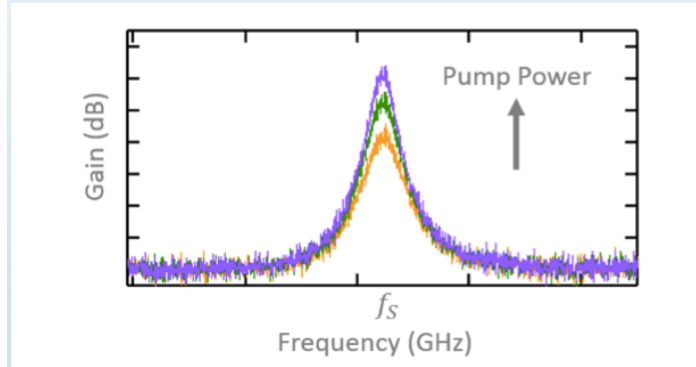
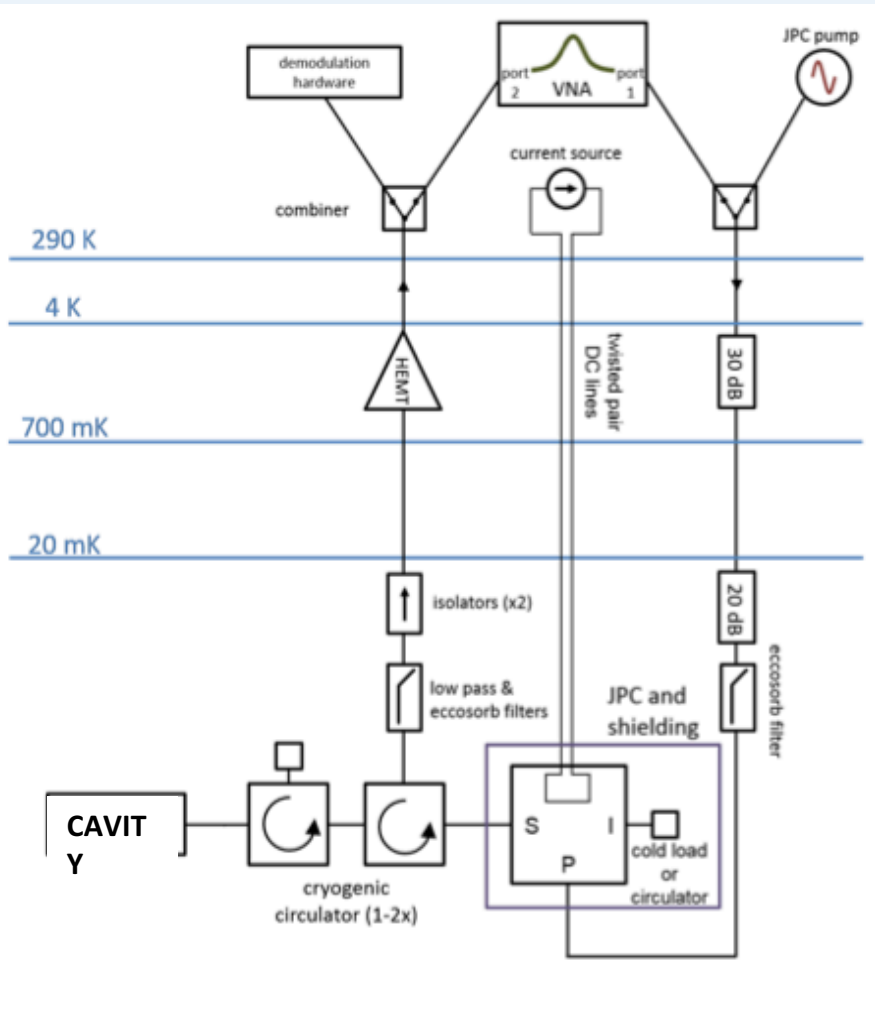
Amplifier

Circulator

Josephson Parametric Amplifier

QCI Yale Spin off Company

$T_{\text{noise}} = 400$ milliKelvin



Working temperature 20 mK

A JPA has been bought with the help of LNL Director and will be soon installed in LNL dilution refrigerator (from AURIGA experiment) now under commissioning

Single Photon Microwave Detector

- The request for the final apparatus is to use a **microwave quantum counter**. World wide researches are under way in this direction outside our collaboration. Contact have been established with a group in Chalmers University that are interested in collaborating with us.

APPLIED PHYSICS LETTERS 103, 142605 (2013)



Underdamped Josephson junction as a switching current detector

G. Oelsner,¹ L. S. Revin,^{2,3} E. Il'ichev,^{1,4} A. L. Pankratov,^{2,3,a)} H.-G. Meyer,¹ L. Grönberg,⁵ J. Hassel,⁵ and L. S. Kuzmin^{3,6}

¹Institute of Photonic Technology IPHT, D-07702 Jena, Germany

²Institute for Physics of Microstructures of RAS, GSP-105, Nizhny Novgorod 603950, Russia

³Laboratory of Cryogenic Nanoelectronics, Nizhny Novgorod State Technical University, Nizhny Novgorod, Russia

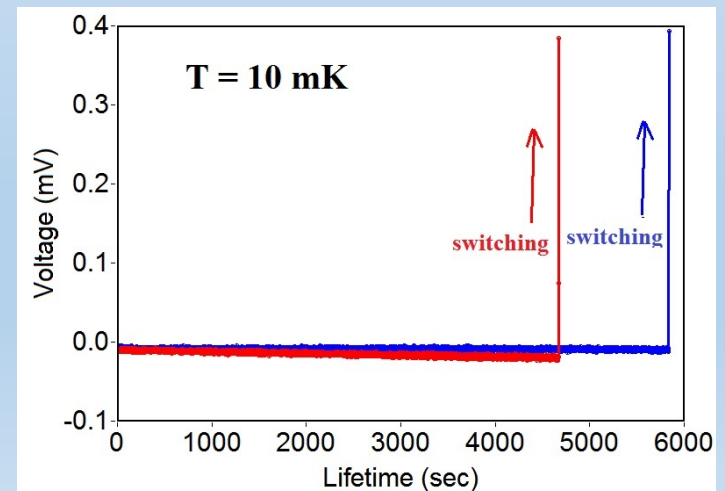
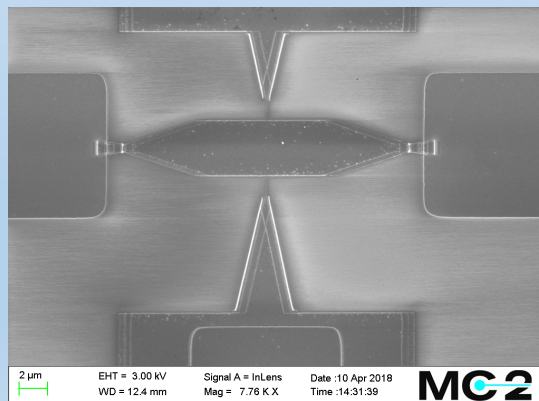
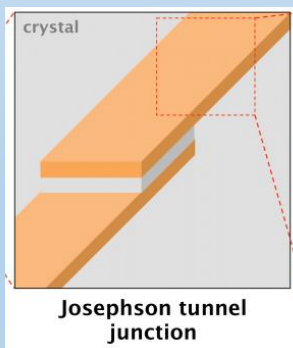
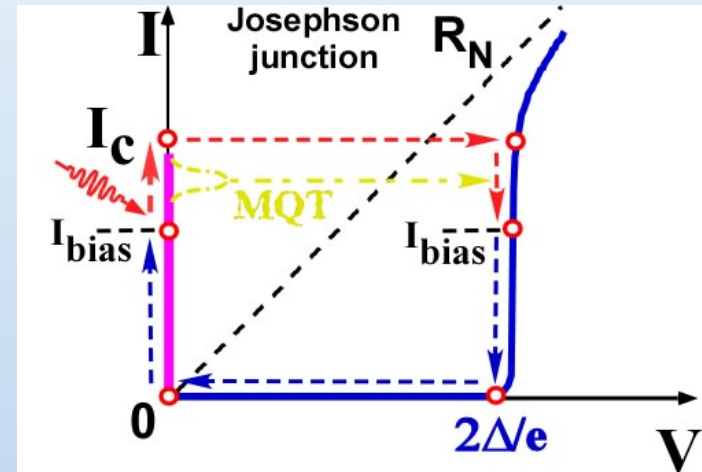
⁴Novosibirsk State Technical University, 20 Karl Marx Avenue, 630092 Novosibirsk, Russia

⁵VTT Technical Research Center of Finland, P.O. Box 1000, FI-02044 VTT, Finland

⁶Chalmers University of Technology, SE-41296 Gothenburg, Sweden

(Received 6 July 2013; accepted 20 September 2013; published online 3 October 2013)

We demonstrate the narrow switching distribution of an underdamped Josephson junction from the zero to the finite voltage state at millikelvin temperatures. We argue that such junctions can be used as ultrasensitive detectors of the single photons in the GHz range, operating close to the quantum limit: a given initial (zero voltage) state can be driven by an incoming signal to the finite voltage state. The width of the switching distribution at a nominal temperature of about $T = 10$ mK was 4.5 nA, which corresponds to an effective noise temperature of the device below 60 mK. © 2013 AIP Publishing LLC. [<http://dx.doi.org/10.1063/1.4824308>]



First results @ 14 GHz with lifetime in excess 10^3 s

Single Photon Counter based on a Josephson Junction at 14 GHz for searching Galactic Axions

Leonid Kuzmin, Alexander S. Sobolev, Claudio Gatti, Daniele Di Gioacchino, Nicolò Crescini, Anna Gordeeva, Eugeni Il'ichev

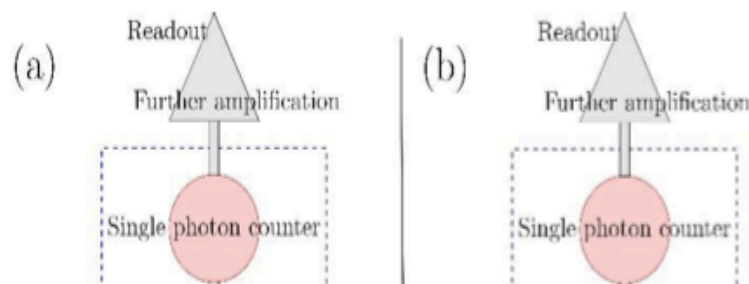
Abstract— Axions and axion-like particles appear in well-motivated extensions of the Standard Model of particle physics and may be the solution to the long-standing puzzle of the Dark Matter in our Universe. Several new experiments are foreseen in the next decade searching them in a wide range of the parameter space. In the mass region from few to several tens of microelectronvolt, detector sensitivity will be limited by the Standard Quantum Limit of linear amplifiers and a new class of single microwave-photon detector will be needed.

We have developed a single photon counter based on the voltage switching of an underdamped Josephson junction that is coupled to a coplanar waveguide. By measuring the switching voltage, we can register single photons at 14 GHz with the rate less than 1 photon per 3000 sec.

Index Terms—Single Photon Counter, Josephson Junction, Axions, Critical current, Coplanar waveguide.

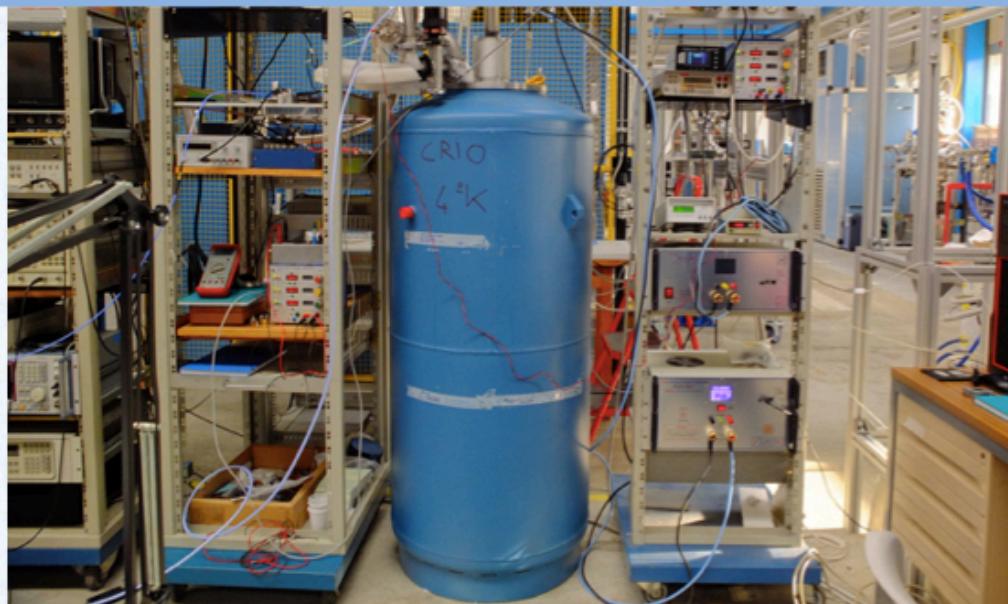
electromagnetic signals. In particular, experiments searching in the mass range from few to hundreds of μeV must be able to detect single microwave photons with a rate of a fraction of Hz and no dark counts.

In the following, we will discuss the requirements for halo-scope searches using the standard axion conversion in a magnetic field (Primakoff conversion), as well as the axion conversion through the interaction with a magnetized media [8]. The detection scheme is schematically shown in figure 1.

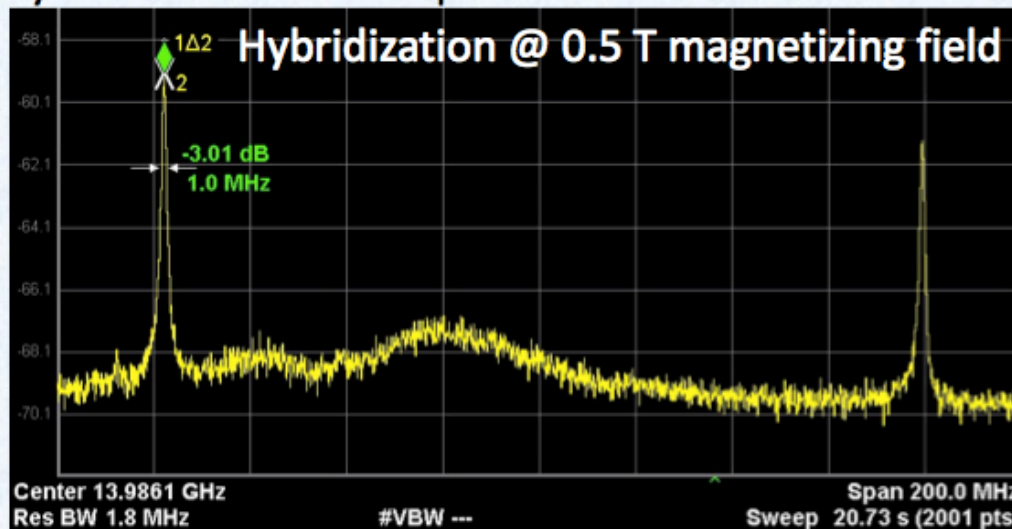


QUAX R&D experimental set-up

- Cylindrical cavity $\nu_c = 14$ GHz (26 mm diameter, 50 mm length)
- 5 spheres of GaYIG – 1 mm diameter – spin density 2.1×10^{28} 1/m³ (measured from coupling/mode separation)
- HEMT amplifier – system noise temperature 9K
- High-precision and stability current generator (up to 20 A \pm 0.3 mA)
- Highly uniform magnetic field (tens of ppm) with superconducting magnet (0.5 T field with 12.5 A)
- Fast ADC for data taking (2 Ms/s) – 16 bit



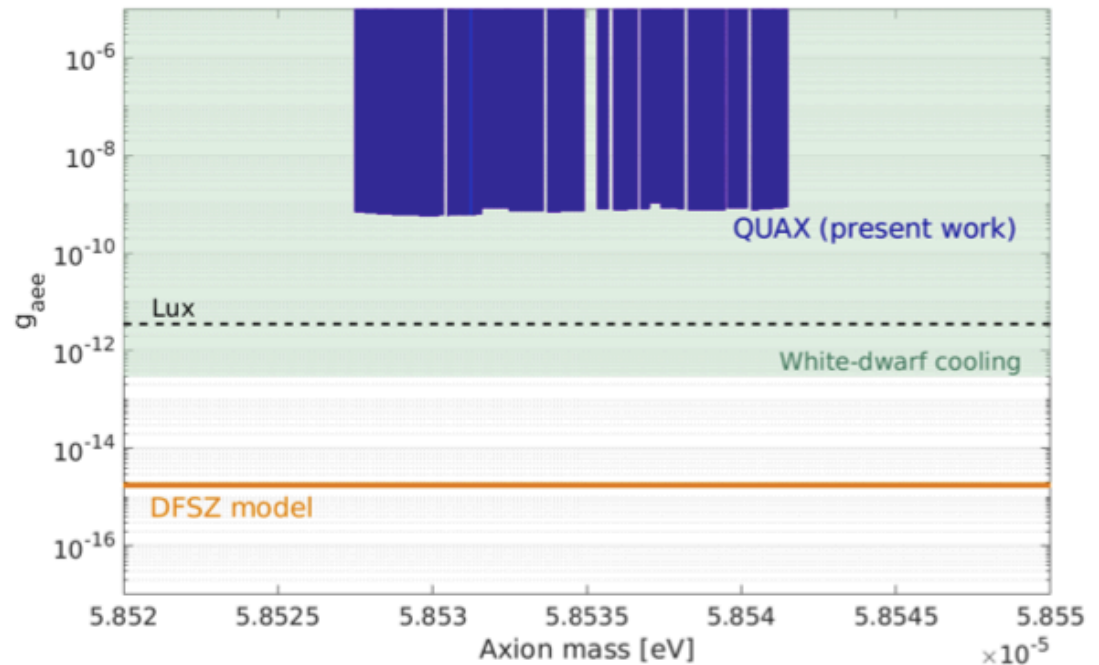
System transmission spectrum



Current sensitivity

Residual power sensitivity can be recast directly into axion coupling, taking also into account the mode Lorentzian shape

$$g_{aee} > \frac{e}{\pi m_a v_a} \sqrt{\frac{2\sigma'_P}{\mu_B \gamma n_a n_s V_s \tau_+}},$$



First limit in the parameter space $\{m_a, g_{aee}\}$ obtained from an experiment searching for axions as the dominant Dark Matter component of Galactic halo

Sensitivity is still poor but:

- Material volume
- System equiv. noise temp.
- Relaxation time

This results
 2.6 mm³
 15 K
 0.1 μs

QUAX R&D (2019)
 42 mm³
 0.2 K
 0.3 μs

QUAX (Goal)
 10⁵ mm³
 counter ($T_{\text{eff}} < 1$ mK)
 2 μs

B1. Up Conversion Scheme (IRQC)

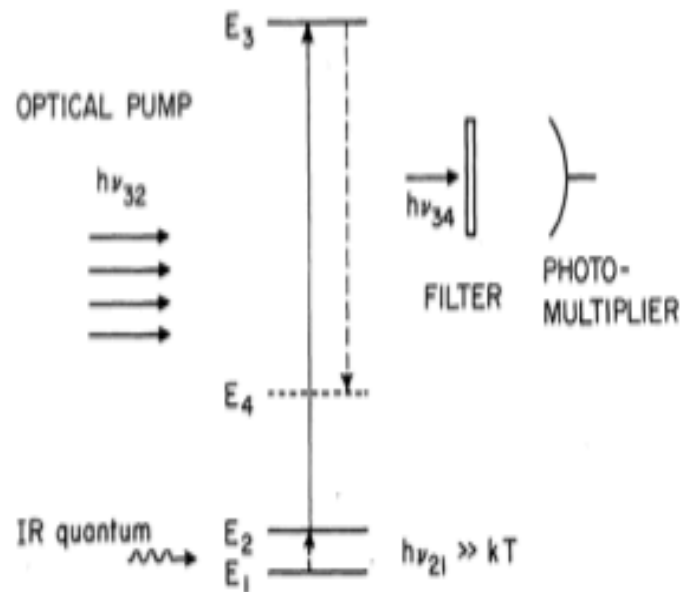
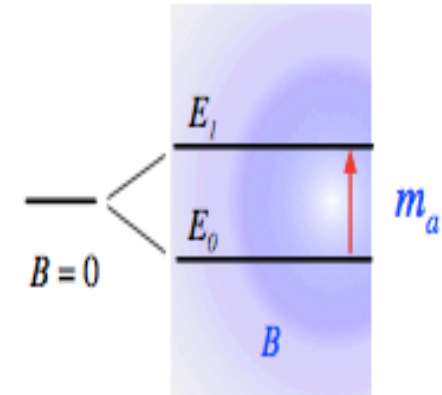
changing strategy for large axion masses m_a

AXION-FERMION interaction

detection of atomic transitions

$|0\rangle \rightarrow |i\rangle$ in which axions are absorbed

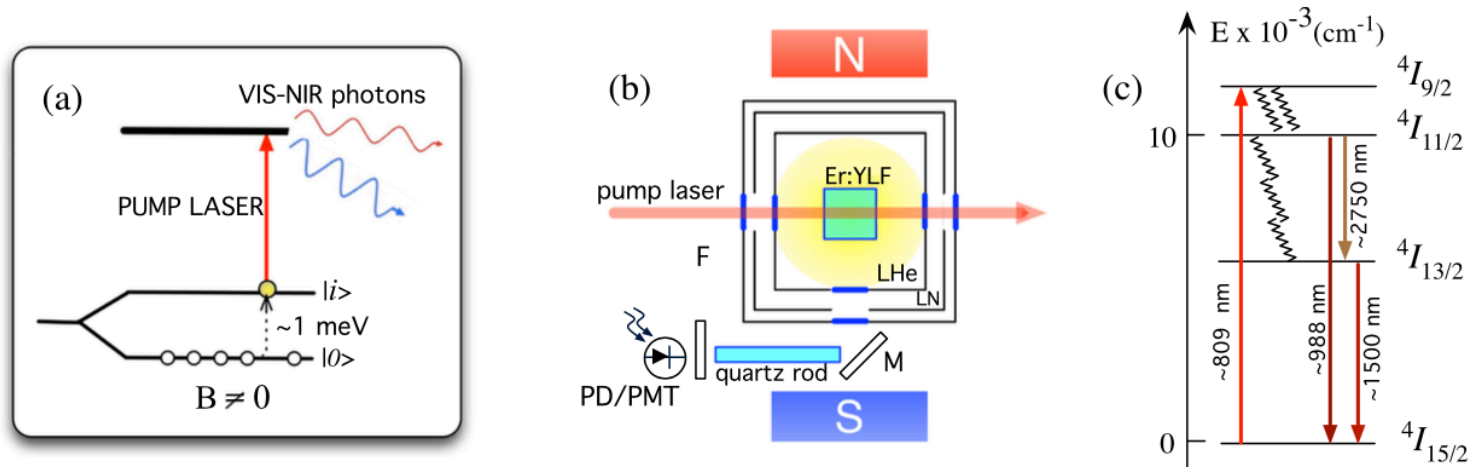
- ▶ QUAX \Rightarrow axions are converted to *magnons*
- ▶ AXIOMA \Rightarrow axions are converted to VIS-NIR *photons*



- pump laser resonant with transition $2 \rightarrow 3$
- material transparent to the pump until an IR photon is absorbed ($1 \rightarrow 2$)
- level 3 is **fluorescent** \Rightarrow detection can be accomplished via conventional detectors (PMT or PD)
- such energy level scheme can be realized in wide bandgap materials doped with trivalent rare-earth ions

N. Bloembergen, *Phys. Rev. Lett.* **2**, 84 (1959)

Axion Detection via Zeeman Up-Conversion Atomic Transitions



$$N_A R_i = 8.5 \times 10^{-3} \left(\frac{\rho_a}{0.4 \text{ GeV/cm}^3} \right) \left(\frac{E_a}{330 \mu\text{eV}} \right)^2 g_i^2 \left(\frac{\sqrt{v^2}}{10^{-6} c^2} \right) \left(\frac{\min(t, \tau, \tau_{\nabla a})}{10^{-6} \text{ s}} \right) \text{ Hz},$$

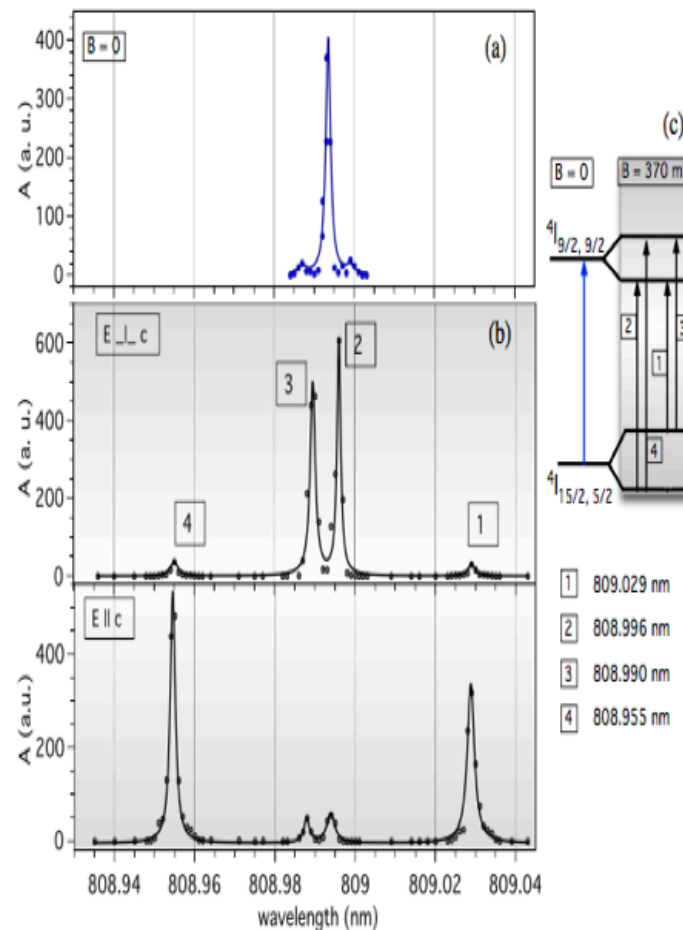
- ▶ axion-induced transitions take place between Zeeman-split ground state levels in rare-earth doped materials
- ▶ transitions involve electrons in the $4f$ shell (as if they were free atoms...)
- ▶ a tunable laser pumps the excited atoms to a fluorescent level
- ▶ crystal immersed in LHe and superfluid He



AXION DETECTION IN RE-DOPED CRYSTALS

→ spectroscopic properties at “high” RE concentration (0.1 %, i.e. $\geq 10^{19}$ axion target electrons/cm³)
in ~ 1 l- active volume

the linewidth of the transition driven by the laser
must be narrower than the energy difference
between the atomic levels $|0\rangle$ and $|i\rangle$



ppm purity level in RE crystals **HARD TO ACHIEVE** to remove Fe & Ni

AXION DETECTION IN RE-DOPED CRYSTALS: TEMPERATURE BEHAVIOUR

Thermal occupation of the Zeeman upper level needs to be suppressed

fundamental noise limit \rightarrow thermal excitation of the Zeeman excited level

$$N_A R_t = \bar{n} / \tau$$

$\bar{n} = N_A \exp(-E_a/kT)$ average number of excited ions in the energy level E_a

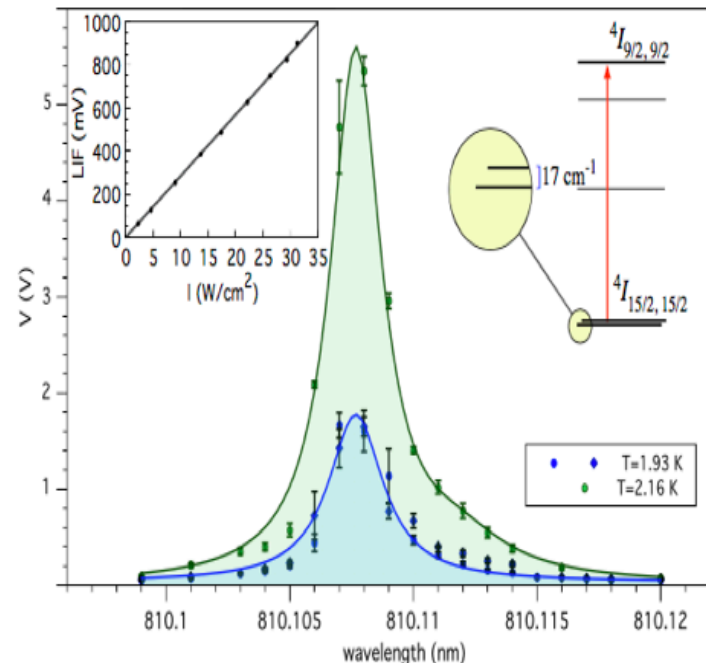
SNR= 3, statistically significant number of counts within $t_m = 1$ h

\rightarrow thermal excitation rate $R_t = 6 \times 10^{-3}$ Hz

$\tau = 1$ ms level lifetime $\rightarrow \bar{n} \leq 5 \cdot 10^{-6}$

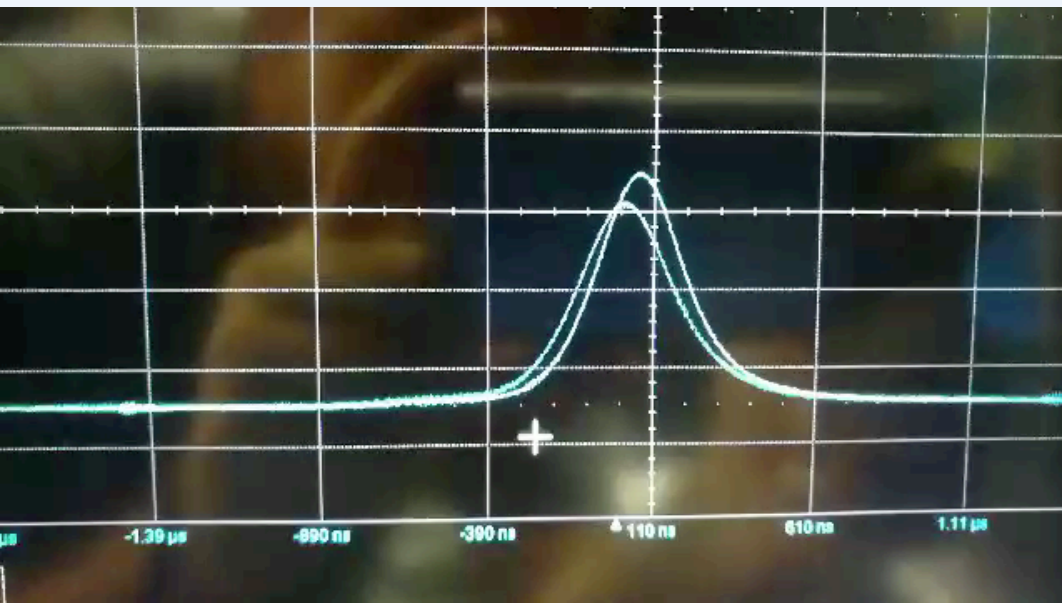
Axions with mass greater than 80 GHz can be searched, provided $T \leq 57$ mK.

\Rightarrow ultra-cryogenic ($T \sim 100$ mK) optical apparatus
Laser-related backgrounds (~ 10 W/cm²)?



The pump laser does not affect the thermal population of the Zeeman excited level [up to a \sim W/cm² intensity]

SUPERFLUORESCENCE PHENOMENA @ 1 KELVIN TEMPERATURE



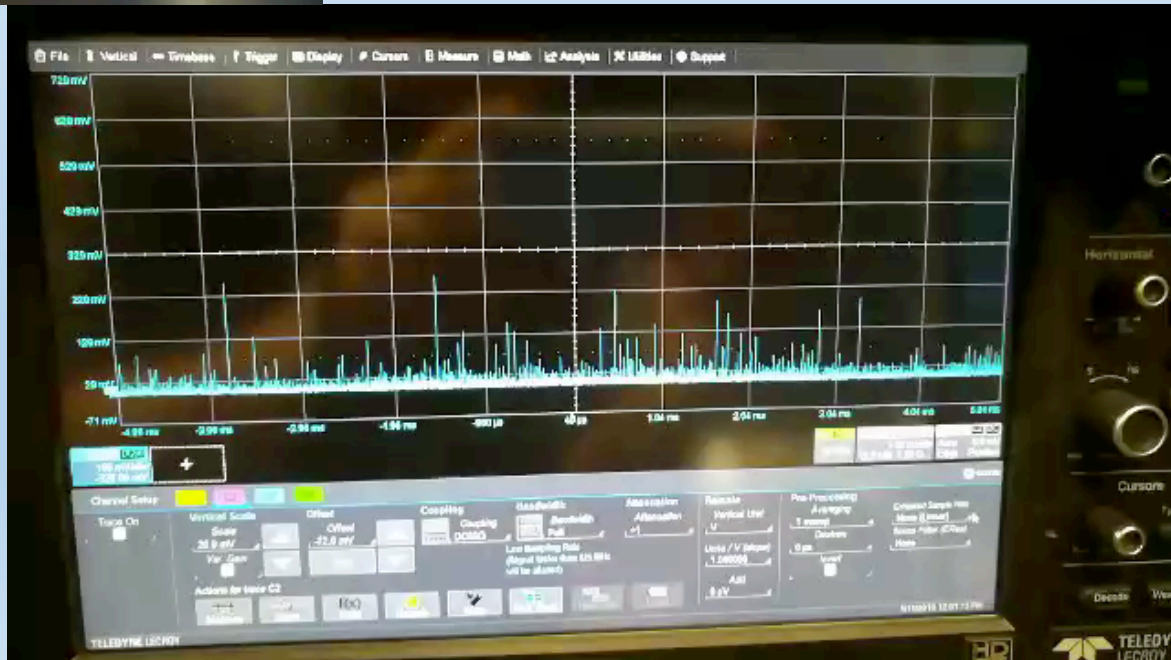
Single Pulse Emission

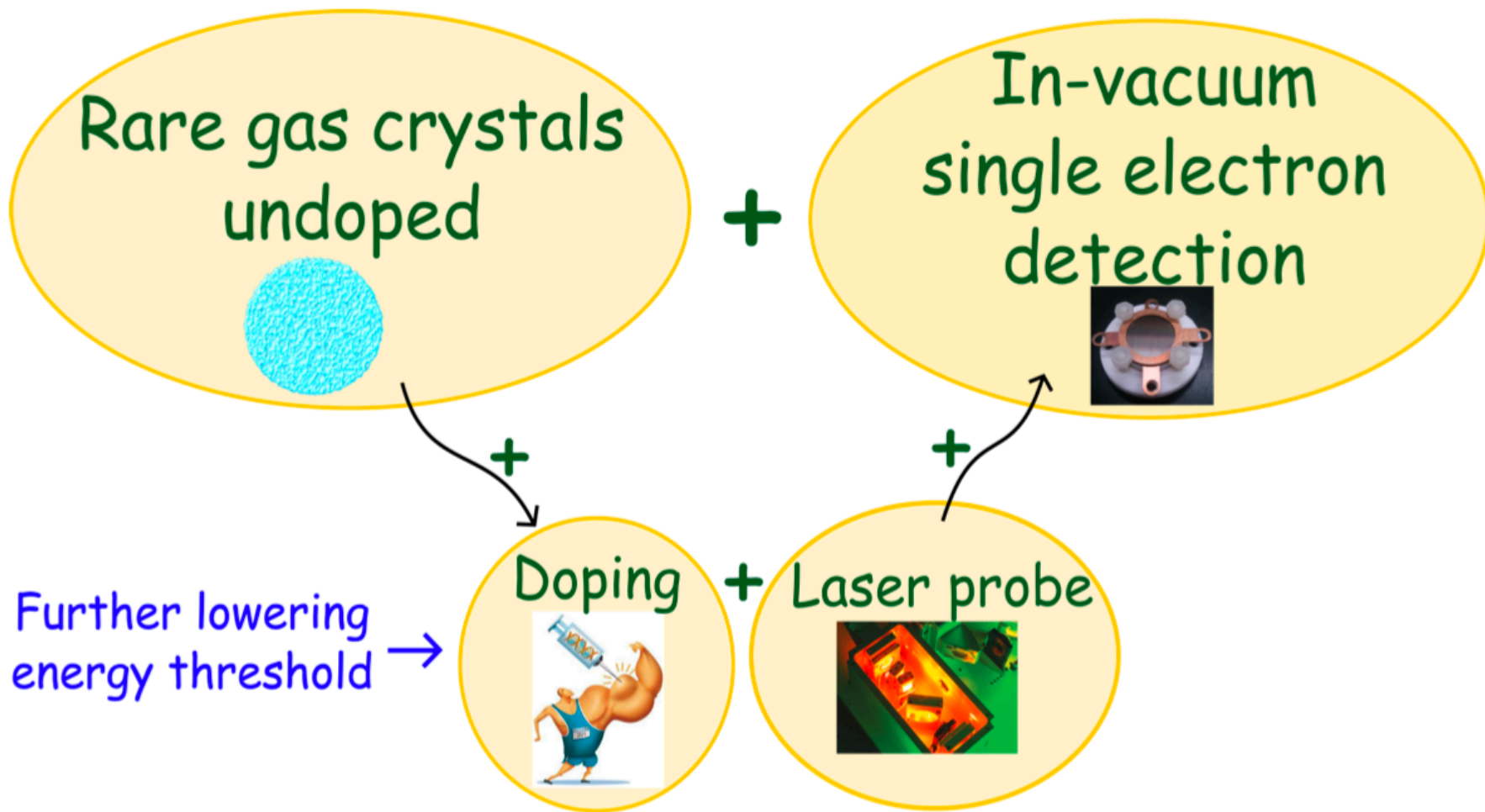
Pulses over Time

Phenomena Under Investigation

Quantum Macroscopic State

Article on the way





Fields:

Cryogenics and low temperature technologies + Solid State (rare gas crystals)
+ high efficiency/low dark count rate Electrons sensors
+ Dopants energy levels + tunable/narrow bandwidth Laser systems

Why Rare Gases crystals?

- ▶ **Matrix Isolation Spectroscopy**: Pimentel in the 50's → studies of free radicals-unstable-transient species (absorption-emission spectroscopy);
- ▶ **low interacting environment** → low line broadening;
 - ▶ feeble interaction host host;
 - ▶ feeble interaction host guest;
- ▶ the species can be **accumulated** in the matrix over many minutes → high density;
- ▶ **large interstitial space** → good doping;
- ▶ (some) has **positive V_0** → good signal;
- ▶ **low melting temperature** → difficult of growing and manipulate;

Some crystal parameters

matrix	Structure	a (pm)	R_{VdW} (pm)	T_{melt} (K)
<i>Neon</i>	ccp	443	158	24.5
<i>Argon</i>	ccp	525	71	84
<i>Krypton</i>	ccp	570	88	116
<i>Xenon</i>	ccp	620	108	161
<i>para – Hydrogen</i>	hcp	470	120	14

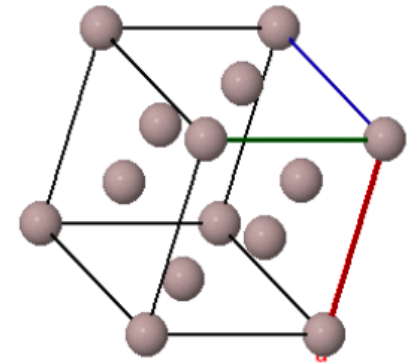
[V. E. Bondybey et al, Chem. Rev. Vol. 96, 2113-2134, (1996)]

[M. L. Klein, J. A. Venables "rare gas solids" Springer (1984)]

Rare gas crystals properties

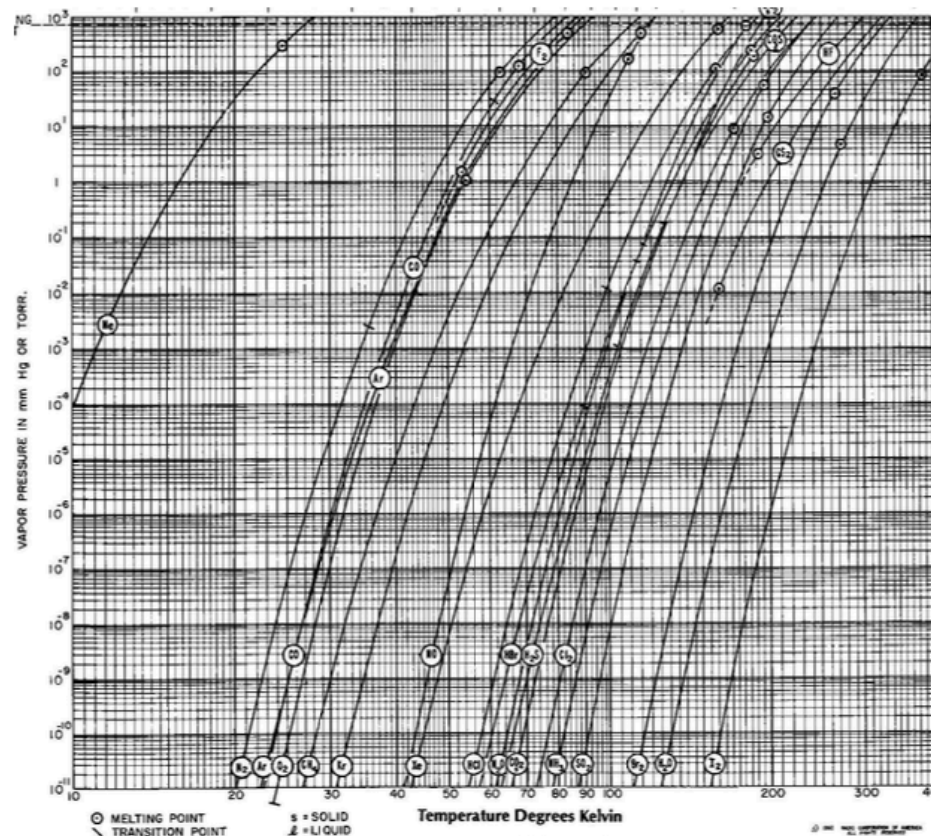
Parameters

matrix	E_{gap} (eV)	V_0 (eV)	μ_e (cm ² /Vs)
Ne	~21.6	+1.1	600
Ar	~14.3	+0.3	1000
Kr	~11.7	-0.2	3700
Xe	~9.3	-0.4@50 K	4500
<i>para</i> - H ₂		+2	

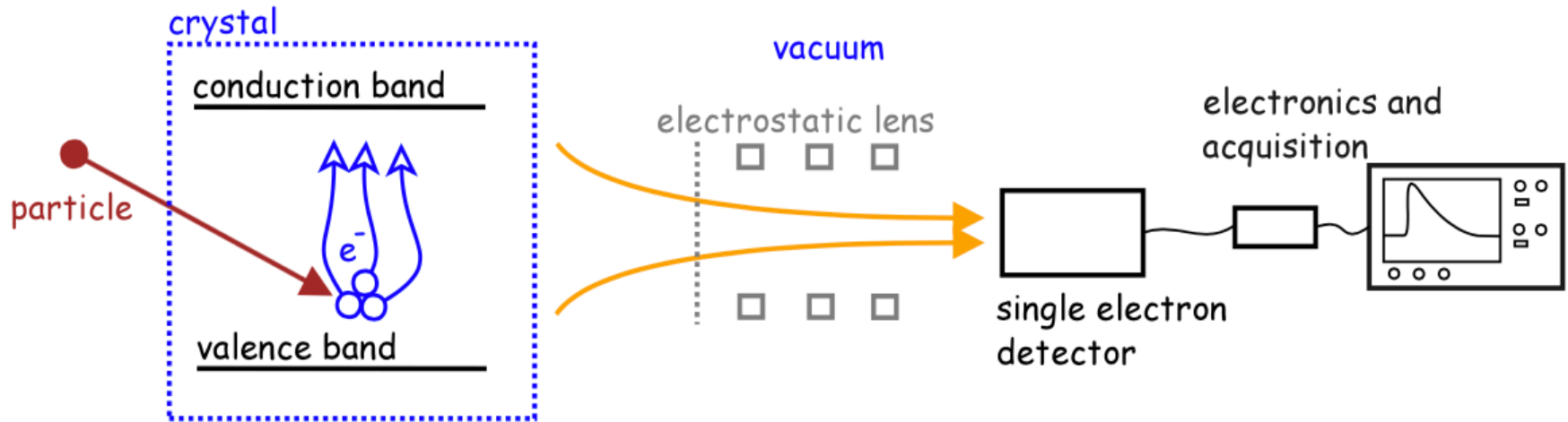


Furthermore, vapor pressure @ low temperature is very low! Worst case: Neon is 10^{-7} mbar at 8K!!!

In solid Argon no space charge problem up to 3000 β /mm²s [V. Brisson et al, Phys. Script. Vol. 23, 688-68, (1981)]



Scheme in undoped matrices



Features:

- Particle **direct ionization**
- Electrons **drift**
- Solid-vacuum interface charge **extraction**
- **In-vacuum charge signal**
- Furthermore UV fluorescence

$$\left. \begin{array}{l} \text{• Particle direct ionization} \\ \text{• Electrons drift} \\ \text{• Solid-vacuum interface charge extraction} \\ \text{• In-vacuum charge signal} \\ \text{• Furthermore UV fluorescence} \end{array} \right\} \Rightarrow E_{th} \sim 100 \text{ eV}$$

- ▶ $\text{Ne} \rightarrow m_W \sim 100 \text{ MeV}/c^2$
- ▶ $\text{Ar} \rightarrow m_W \sim 300 \text{ MeV}/c^2$
- ▶ $\text{Xe} \rightarrow m_W \sim 500 \text{ MeV}/c^2$

- ▶ nuclear recoil;
- ▶ solid-vacuum extraction;

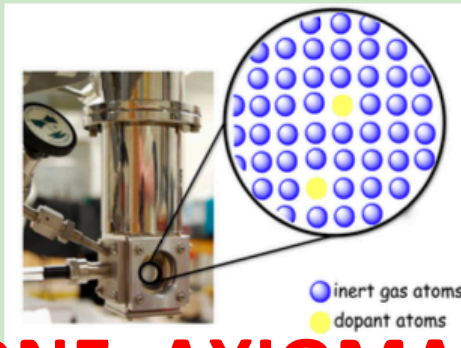
- ▶ high gain e^- detector;
- ▶ low dark count e^- sensors;

Two methods:

- Vapour deposition

Films ($\sim\text{cm}^3$)

- ▶ spray deposition through nozzle;
- ▶ easy doping;
- ▶ pulse tube He cryocooler @4K;
- ▶ $P_{\text{chamber}} \sim 10^{-8}$ mbar;
- ▶ $P_{\text{growth}} \sim 10^{-5}$ mbar;
- ▶ time of growth $\sim 1 \text{ cm}^3 / 2$ hours;
- ▶ annealing;

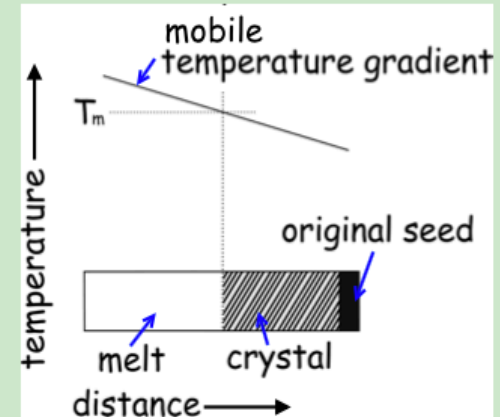


DONE: AXIOMA

- Liquid freezing

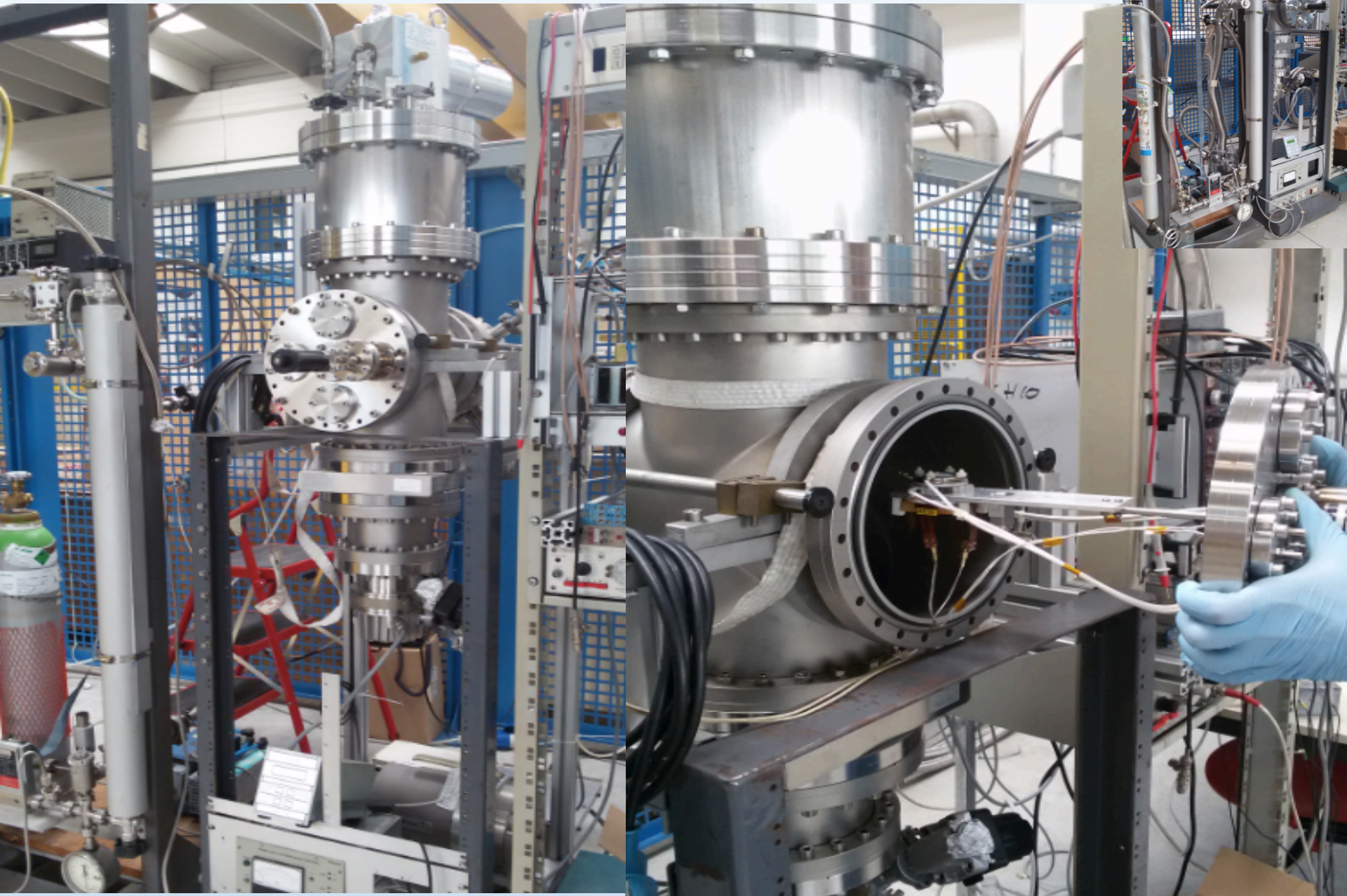
Large crystals ($\sim\text{litres}$)

- ▶ Bridgman-Stockbarger technique;
- ▶ low temperature system:
 - ▶ cryogenic liquids;
 - ▶ pulse tube refrigerators;
- ▶ fine tuning temperature control;
- ▶ time of growth $\sim 1 \text{ dm}^3 / 5$ hours;

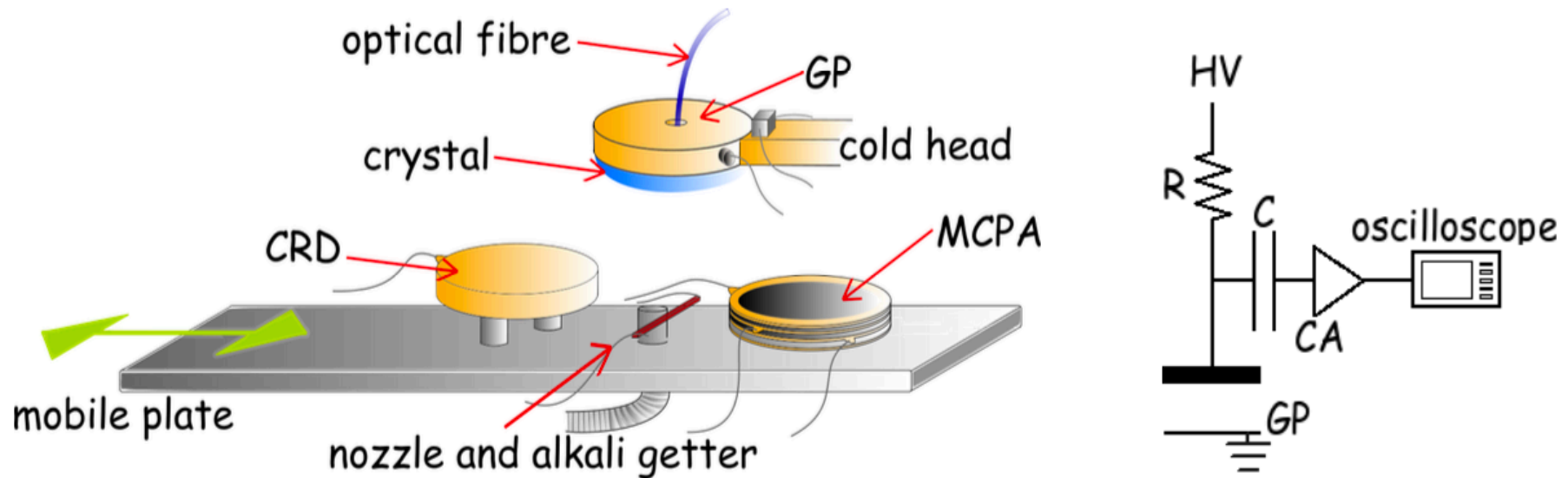


criticism: single crystal VS polycrystalline structure

Experimental Apparatus @ LNL

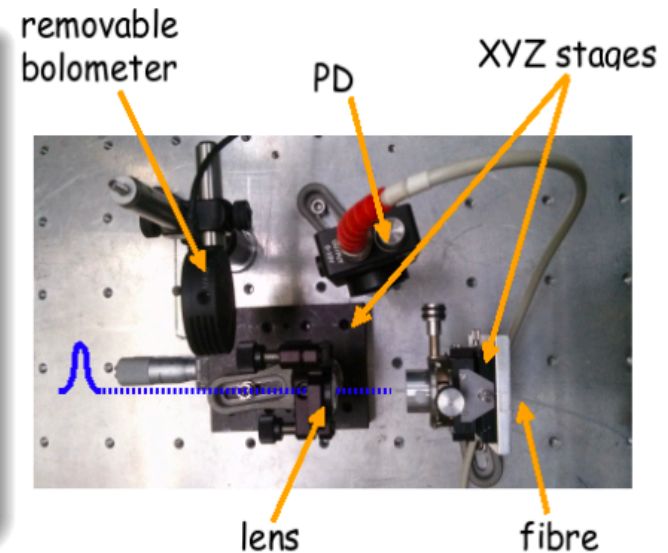


Electrons injection, extraction & collection from a Neon crystal: apparatus

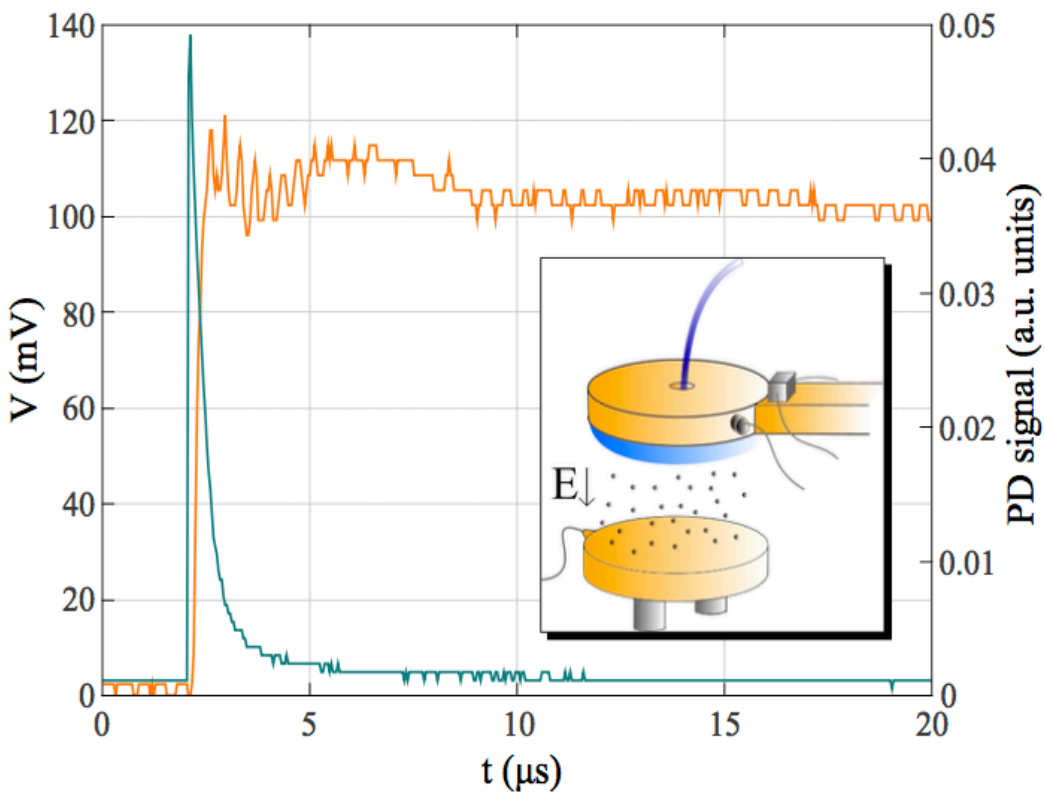


Characteristics

- ▶ Au photocathode in the cold head;
- ▶ fused silica fibre;
- ▶ 10 ns laser pulses @ 266 nm (trigger);
- ▶ energy up to 1 mJ;
- ▶ charge receiver disk or microchannel plate assembly;

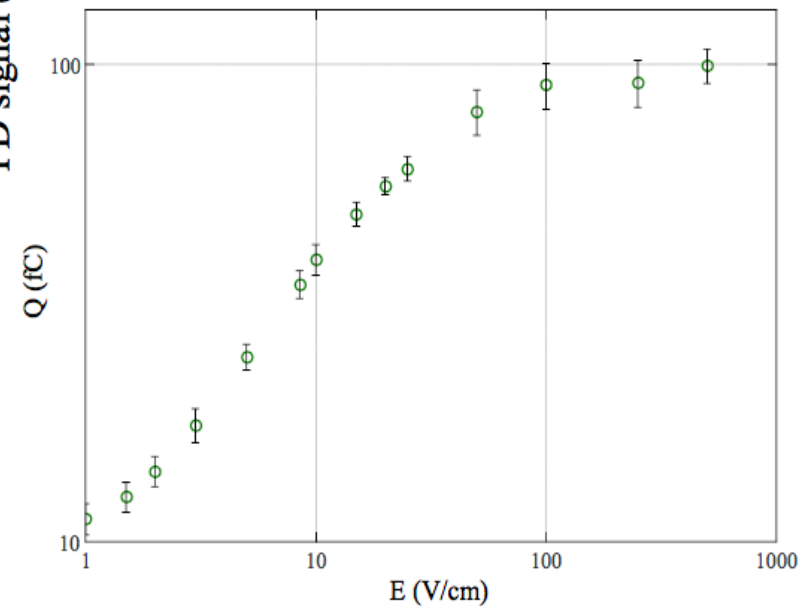


Electrons extraction from a Neon crystal: signal



Measurements:

photoelectrons injection and emission in 2 mm thickness Ne for different electric field applied



long time (hours) stability signal



no space charge effect!



no trapping sites!

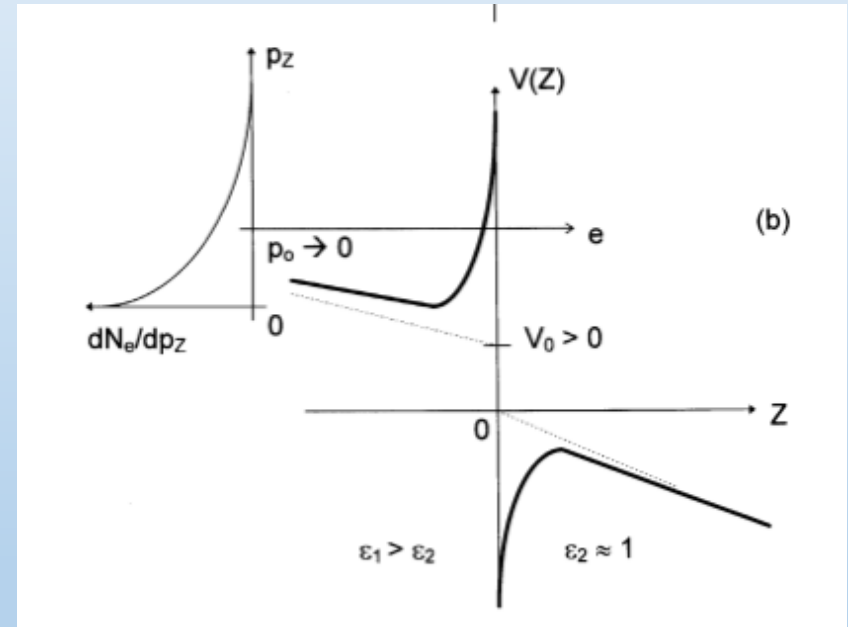
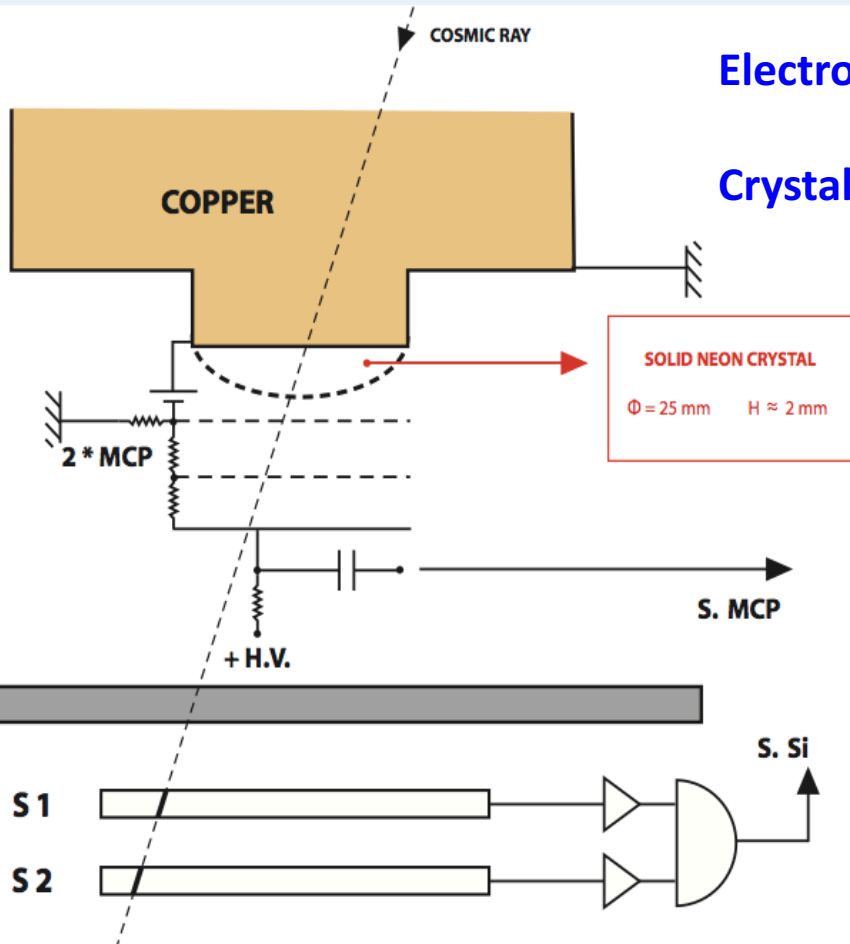


high quality crystals!

Solid Neon: Cosmic Ray Detection Set up

Electron Tunnel through Neon-Vacuum Barrier

Crystal Volume : 25 mm Diameter , 2 mm Height



Estimated Energy Threshold tens of eV: W Neon Value (MCP Low Dark Count Rate $< 10^{-2}$ Hz)

Solid Neon: Cosmic Ray Detection

$P_{\text{solid neon/vacuum @4Kelvin}} < 10^{-7} \text{ mbar}$, $V_{0 \text{ tunneling}} = +1.1 \text{ V}$, $\rho_{\text{neon}} \approx 1,2 \frac{\text{gr}}{\text{cm}^3}$

Electron Mobility $2000 \text{ cm}^2/\text{Vs}$ @ 4 Kelvin , Hopping Ionic Conduction

Single Electron Sensitivity via MCP , Deep UV Scintillation Present



Silicon Detector Trigger

MCP Signals :

Around 100 electrons signal

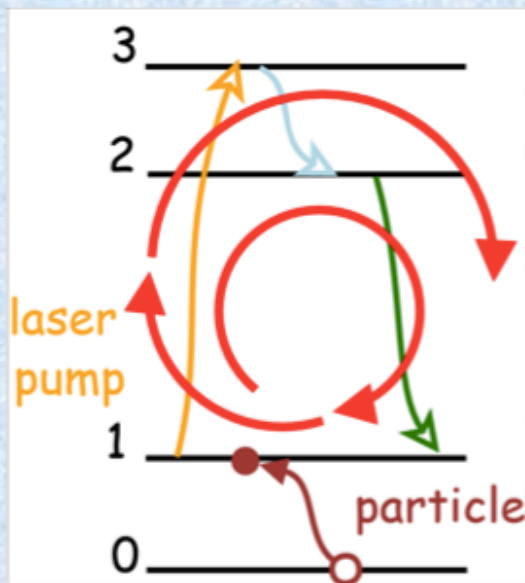
Electron in vacuum could be
Transported far away from Solid

**Sensitivity at Weak Cross Section Level
for a few Kg Target material**

B) Fluorescence Recycling Phenomena in doped cryogenic crystals

Matrix isolated crystals: RE, alkali or nitrogen doped

- Exploit internal energy level scheme
- Narrow bandwidth laser pump probing
- Fluorescence signal emission



- Particle: transition 0-1
- Laser: transition 1-3
- Non-radiative decay: transition 3-2
- Fluorescence signal: transition 2-1

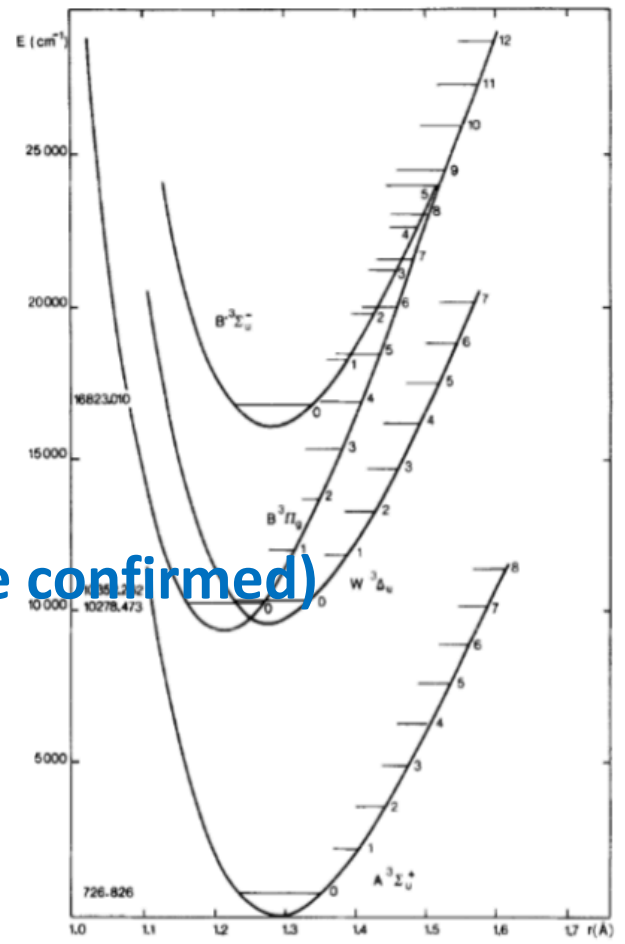
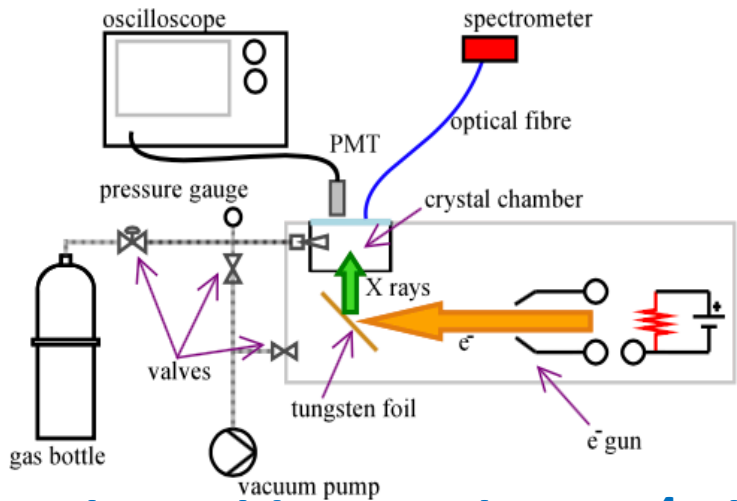
A single particle transition triggers

N fluorescence photons emission

Recycling efficiency $\approx N_{\text{photons}} \tau_1 \sigma_{13} \beta_{21}$ \longrightarrow high efficiency detector in **eV range!**

Radio-luminescence in solid Nitrogen:

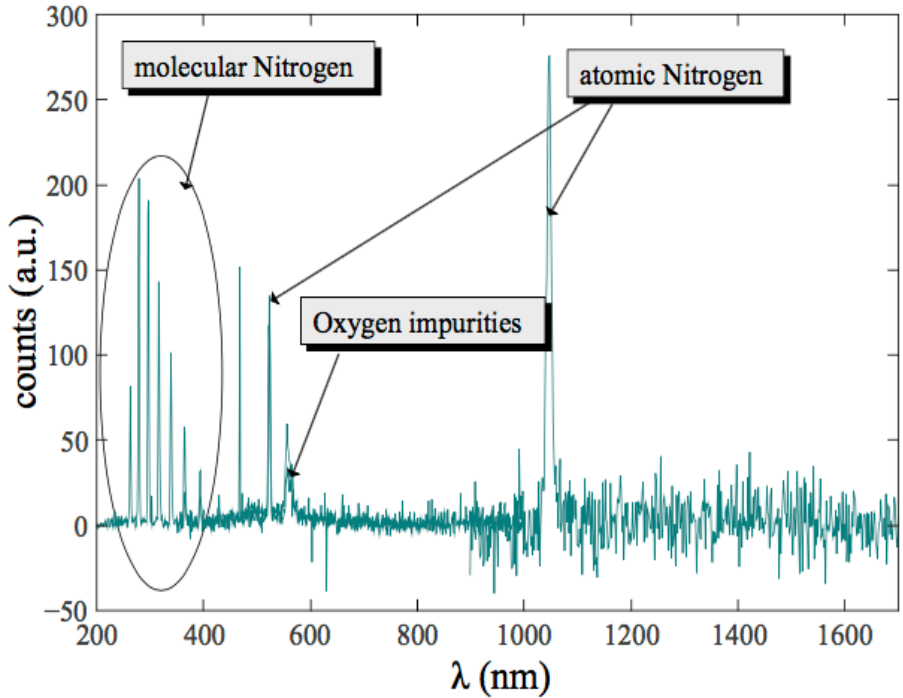
- ▶ 60 keV electrons;
- ▶ Tungsten target;
- ▶ 10 K Nitrogen crystal;



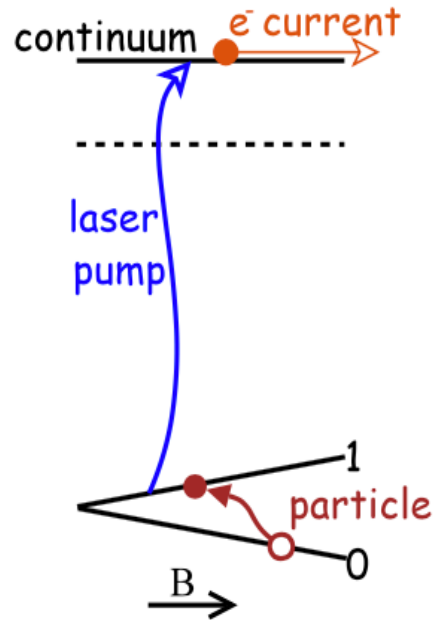
long lifetime of 1st excited level: ~ 3 s!!!

[G. Zumofen et al. J. Chem. Phys. 81, 2305 (1984)]

Light Yield more than 10^4 photons/MeV (to be confirmed)



Scheme in doped matrices



Features:

- Internal energy levels
- Incident energy is absorbed
- laser induced ionization LII from excited level
- solid-vacuum electron extraction
- in-vacuum charge signal
- up-conversion efficiency $\eta = \sigma_{13}\tau_1\phi_L \rightarrow \sim 1$

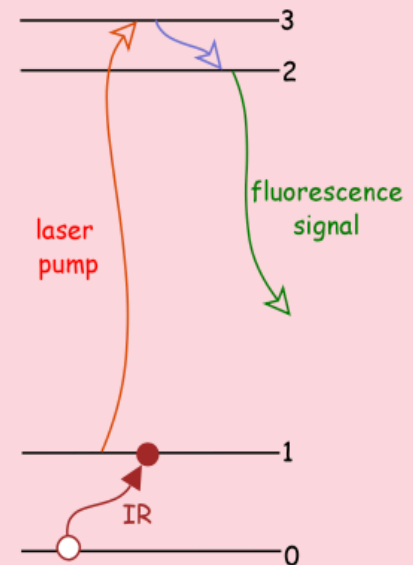
} $\Rightarrow E_{th}: \text{sub-eV}$

Possible application: AXION

- ▶ axion mass: m_a tuned to the $0 \rightarrow 1$ transition ($E_1 - E_0$);
- ▶ Zeeman transition $0 \rightarrow 1$: $\Delta E \sim \mu_B \mathbf{B} \sim (10-1000)\text{meV}$ for $\mathbf{B} < \text{Tesla}$;
- ▶ $K_B T < \Delta E$ required;
- ▶ $R_a \propto m_a^2 V_s N_s \tau_a$

V_s : sample volume; N_s : electron density; m_a and τ_a : mass and coherence time of axion

Bloembergen IRQC!



Possible dopants

Requests:

- ▶ narrow line-width;
- ▶ photo-ionization steep;
- ▶ low interaction with matrix;
- ▶ long lifetime;

Alkali

RE

Possibilities:

Alkali

element	E_{ioniz} (eV)	λ_{ioniz} (nm)
<i>Li</i>	5.39	230
<i>Na</i>	5.13	241
<i>K</i>	4.34	285
<i>Rb</i>	4.17	297
<i>Cs</i>	3.89	318

Rare Earth (RE)

element	E_{ioniz} (eV)	λ_{ioniz} (nm)
<i>Pr</i>	5.47	226
<i>Nd</i>	5.52	224
<i>Sm</i>	5.64	219
<i>Ho</i>	6.02	205
<i>Er</i>	6.10	203

Possible problems:

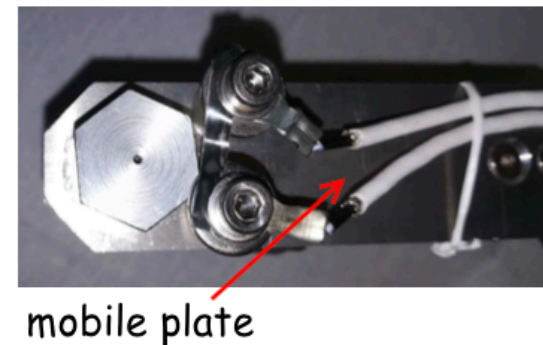
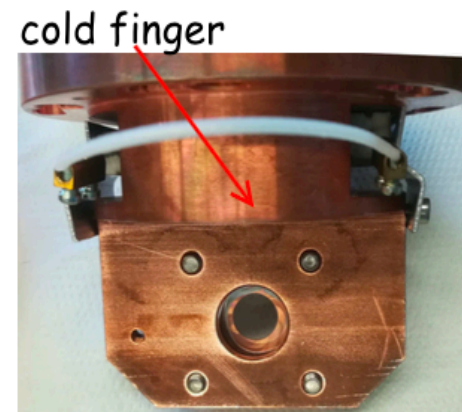
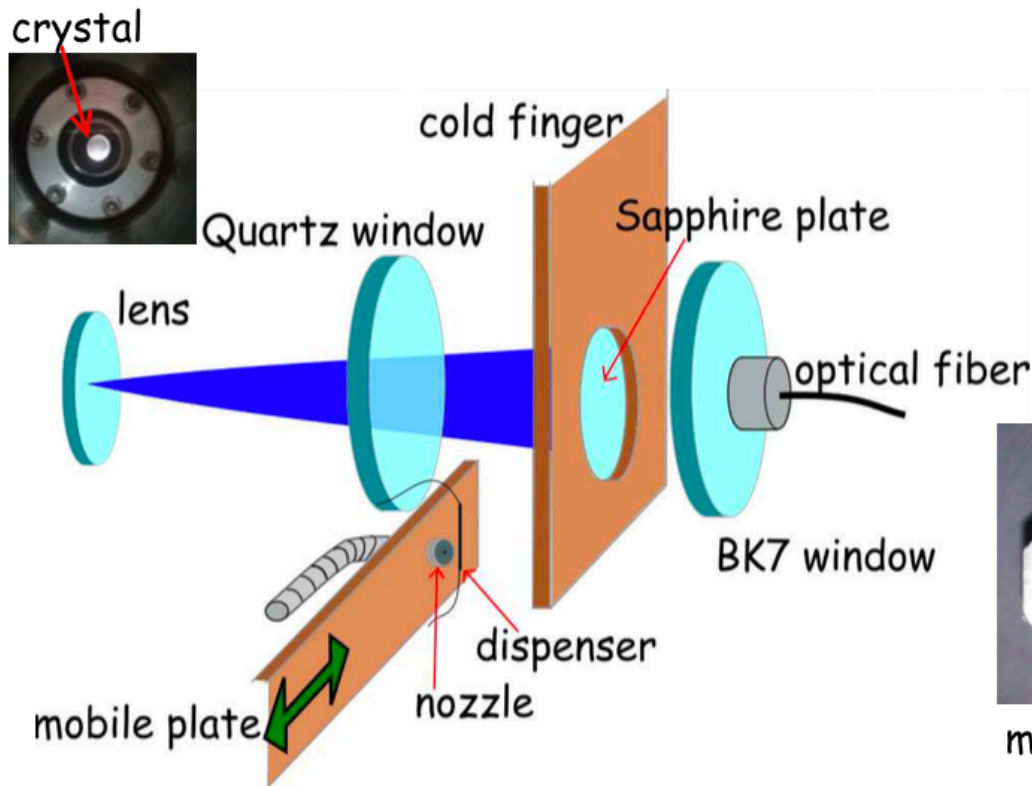
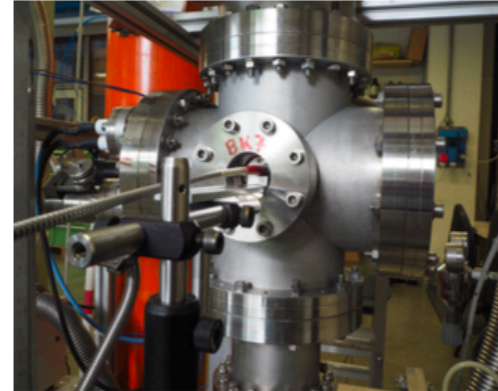
- clustering;
- line broadening;
- impurity;
- interstitial/substitutional sites;

Doped films: apparatus

Crystal size: 2 mm height 25 mm diameter

Apparatus:

- ▶ thin films (\sim mm thickness);
- ▶ transmission measurements (UV-IR):
 - ▶ absorption spectroscopy;
 - ▶ emission spectroscopy;



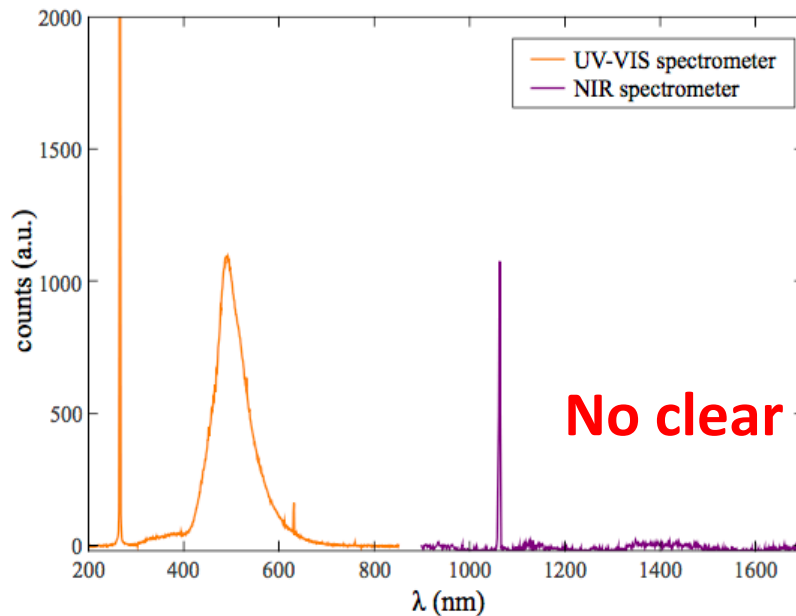
Neon Neodymium: light signal

Excitation:

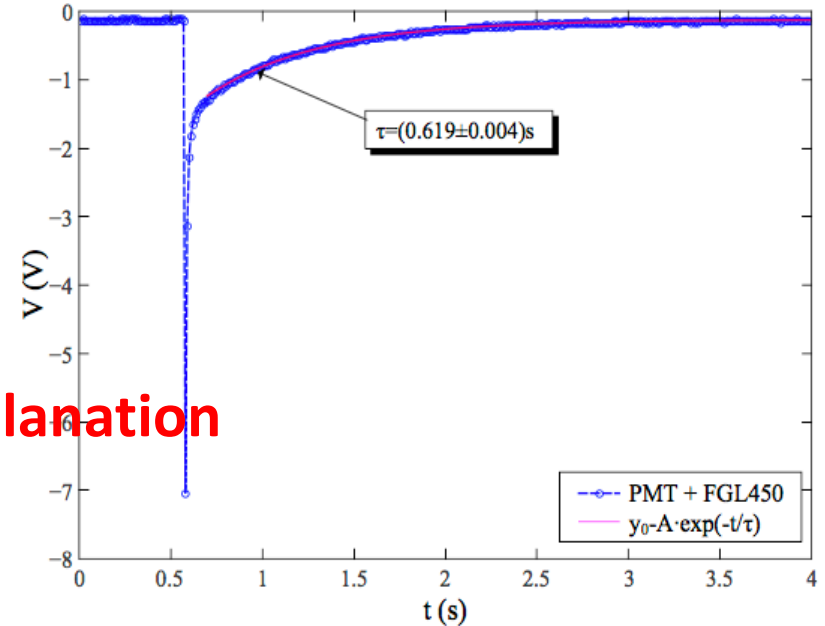
- ▶ 266 nm laser pulses (4.66 eV);
- ▶ length ~ 10 ns;
- ▶ energy ~ 1 mJ;
- ▶ rate ~ 1 Hz;

Detection:

- ▶ UV spectrometer;
- ▶ VIS spectrometer;
- ▶ NIR spectrometer;
- ▶ PMT+pass-band filter;



No clear explanation



Emission spectrum

broad band emission @ ~ 500 nm

Signal lifetime

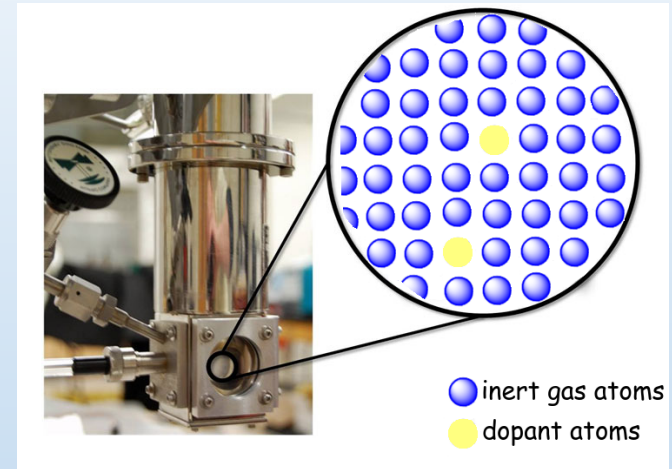
$\tau \sim 0.6$ s

Conclusions: Piero Legacy

- I wish to thank all the people of QUAX and AXIOMA experiments
- Physics need new Instruments/sensors to look ahead:
Otherwise same fishes with the same baits
- PIERO SUPPORT: fundamental to open “ MY ” Legnaro Lab. Activities
- PIERO MODEL: try to involve people and making integration effective at all scales
- PIERO AS A PHYSICIST: Open mind: Is it possible to check? Then try it!
- We take a lot of fun putting our hands and mind into unexplored fields thanks mainly to INFN

Low Energy Threshold Cryogenic Detectors

Future efforts on Cryogenics Noble Gases Matrix Isolation detectors:
Undoped & Doped crystals



3 main approaches proposed:

- A) Single Electron Detection promoted without and with laser and Electric Field with a Kg mass detector via Bridgeman's growing technique
- B) Fluorescence Recycling Phenomena in doped cryogenic crystals
-doping atoms: Rare earth, molecular nitrogen or Alkaline atoms
- C) Inverse Bremsstrahlung electron acceleration under Laser Field combination of electron and light multiplication present in high density media

Comment on Oxide , Fluoride & Chloride doped Crystals

Sappi prendere la tua parte di mondo che ti appartiene

Piero Dal Piaz 1990

- Laser Based coherent scintillators
- Superfluorescent phenomena and two neutrinos emission
- Dirac-Volkov equation and Electron Capture possible experiment
- Inverse brehmstralung in high dense media and some neutrino surprise (at lesat for me)

Novel Detectors Ideas Working in Progress

Giovanni Carugno
INFN & UNIPD

- **Brief Overview: Theory vs Experiments**
- **Detection Strategies**
- **Axion-Photon coupling experiments: Haloscope, Helioscopes, Light Shining Wall**
- **Axion-Electron coupling experiments: Haloscope**
- **Fifth Force type of Experiment**

Sappi prendere la tua parte di mondo che ti appartiene

Piero Dal Piaz 1990

New Class of Laser-Based Detectors

Low Threshold Detectors: from 1 meV to 100 meV

- detection based on laser driven transitions in active media

Zeeman Magnetic type M1 Transition Detection:

A) Infrared Quantum Counter (Bloembergen Idea)

Rare Earth or Transition Metals doped crystals

Fluorescence Photon Detection

B) Matrix Isolation Spectroscopy (New approach)

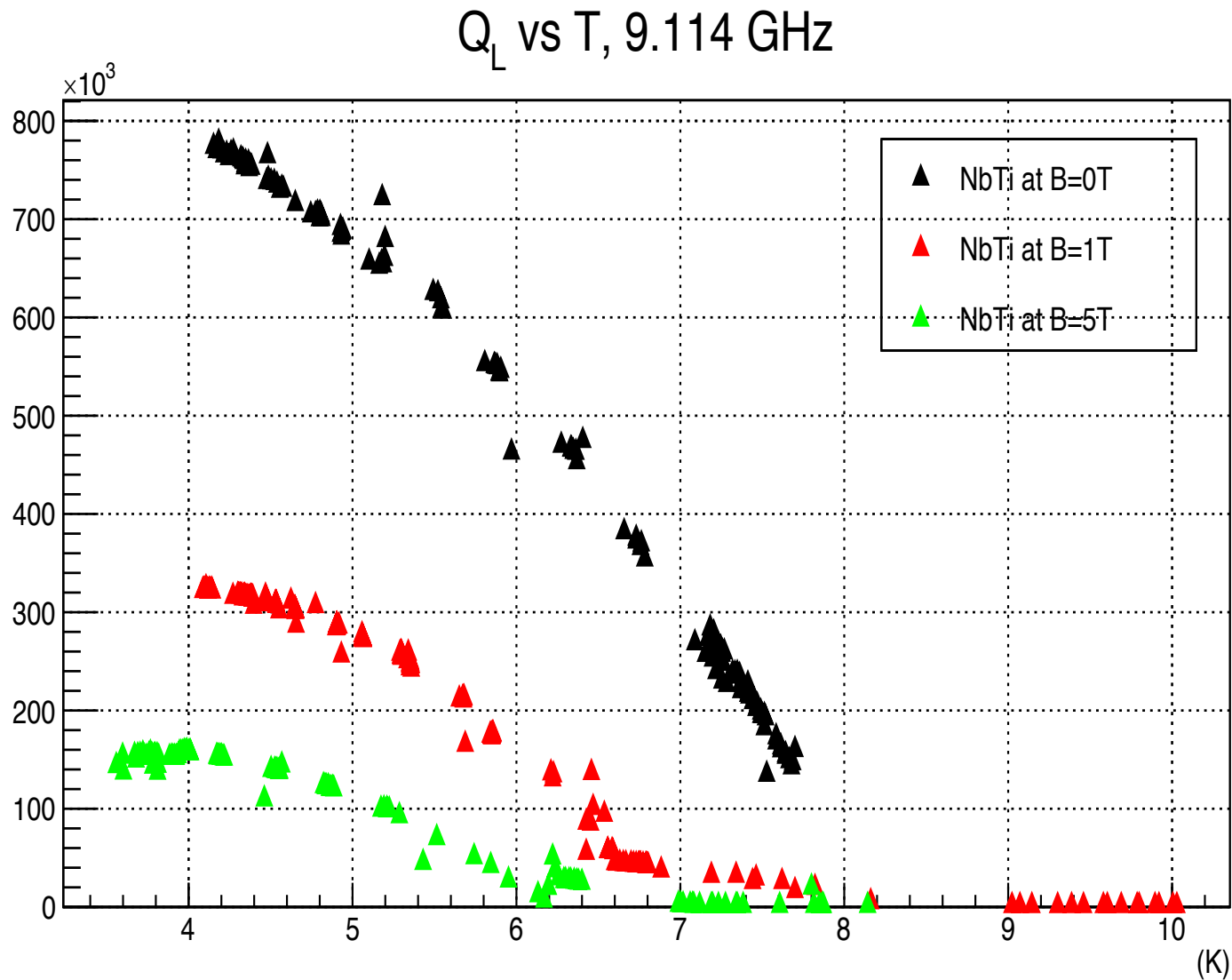
Solid Neon/Methane/Para-Hydrogen Matrix Crystal
doped with Alkaline Atoms

(host atoms retain **almost** the structure of free atoms)

Single Electron Detection

C) Laser Based Scintillators

Q_{loaded} vs Temperature and Field

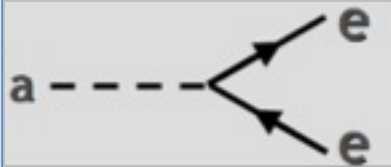


Axion Detection through Zeeman Transition

Exploit the axion-electron coupling

$$L_{ae} = \frac{C_e}{2f_a} \bar{\Psi}_e \gamma^\mu \gamma_5 \Psi_e \partial_\mu a$$

$$C_e \leq 10^{-13} \text{GeV}^{-1}$$



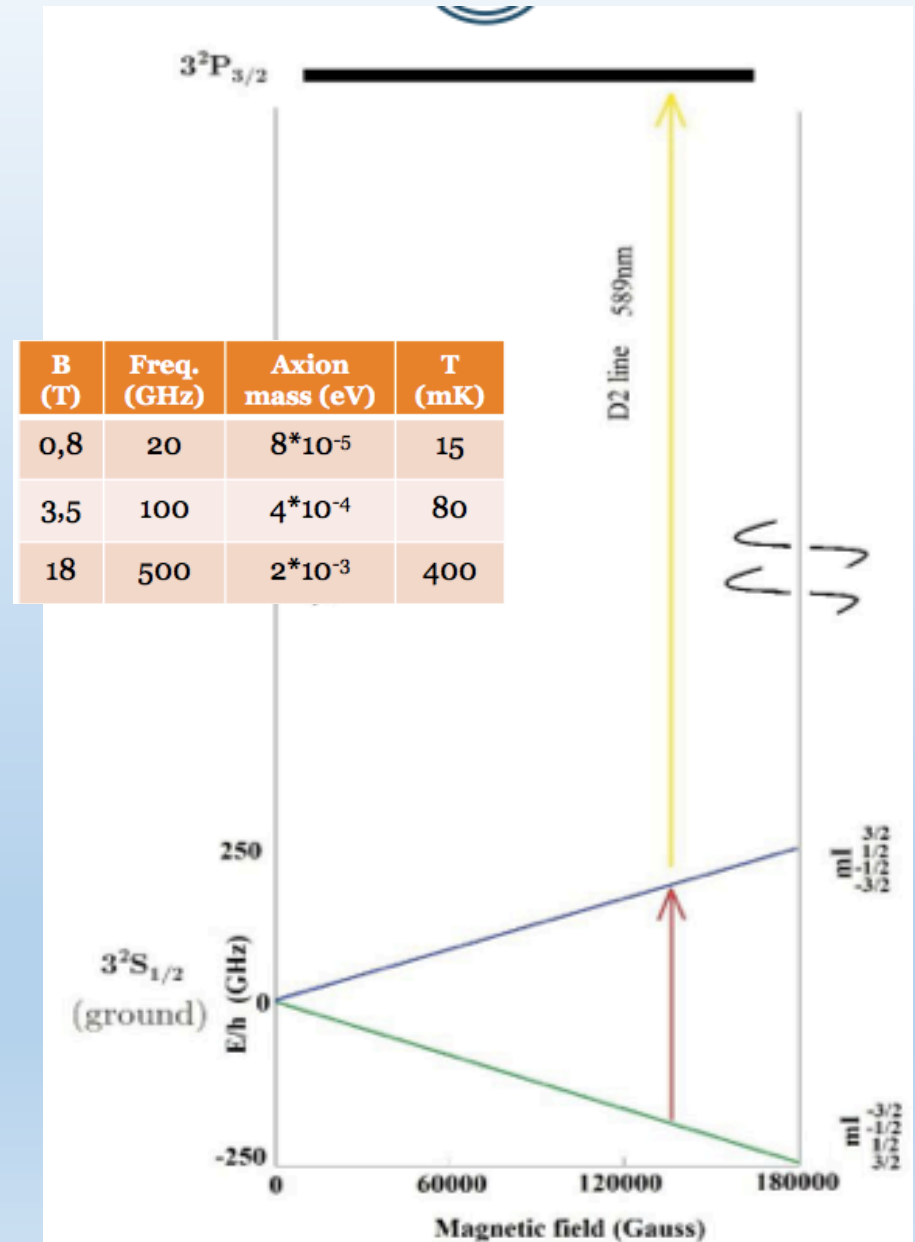
$$H_a = -\vec{S} \cdot \left[\frac{g_p}{m_e} \nabla a \right]$$

(only DFSZ axion)

Axion wind equivalent to effective B

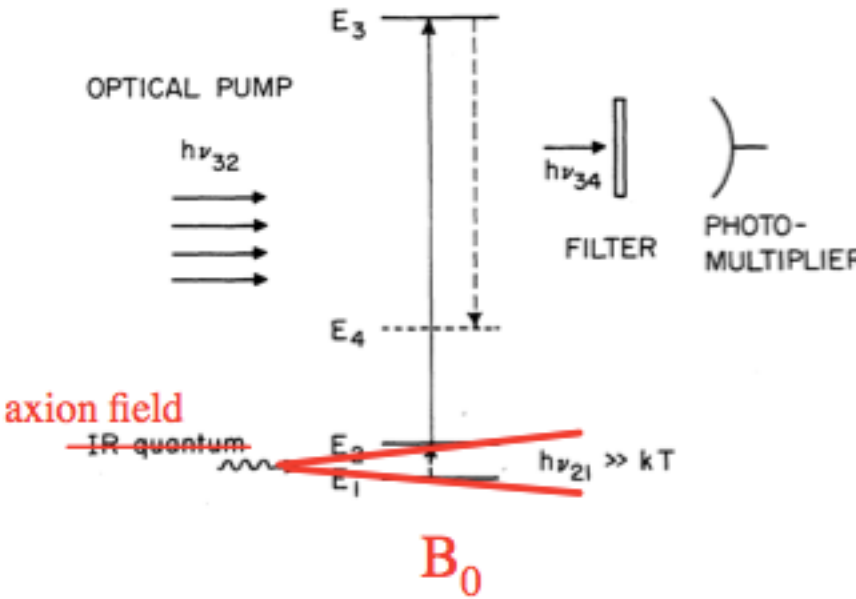
$$B_E = \frac{2g_p}{e} \frac{g_a}{g_J} \nabla_z a$$

$$B_{Ef} \approx \left(\frac{m_a}{10^{-4} \text{eV}} \right) 9.4 \times 10^{-23} T$$



B2. Up Conversion of Zeeman Transition

- material transparent to the pump until an **AXION** is absorbed ($1 \rightarrow 2$)
- transition $1 \rightarrow 2$ takes place between **GS ZEEMAN-SPLIT LEVELS** to allow for tunability (B_0 field) in the interesting axion mass range
- level 3 is fluorescent \implies detection can be accomplished via **IR single photon detectors**
- dopant (rare-earth ion) concentration compatible with transition rate by axion absorption R_i for a **MOLE** of target atoms:



$$\begin{aligned}
 N_A R_i &= g_i^2 N_A \bar{v}^2 \frac{2\rho_a}{f_a^2} \min(t, t_1, t_a) \\
 &= \frac{2.13 \times 10^3}{\text{sec}} \left(\frac{\rho_a}{\text{GeV/cm}^3} \right) \left(\frac{10^{11} \text{ GeV}}{f_a} \right)^2 \\
 &\quad \cdot g_i^2 \left(\frac{\bar{v}^2}{10^{-6}} \right) \left(\frac{\min(t, t_1, t_a)}{\text{sec}} \right)
 \end{aligned}$$

P. Sikivie, PRL 113, 201301 (2014)

Doped Paramagnetic Optical Crystals

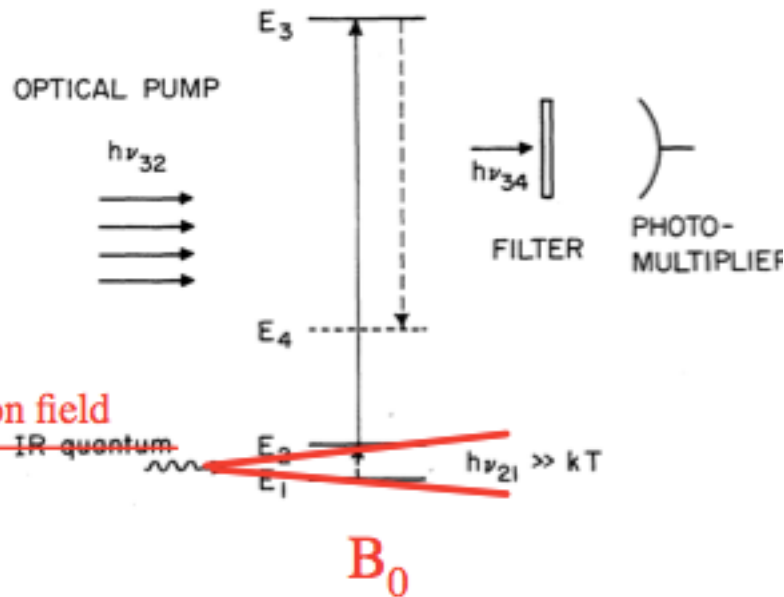
1% \longleftrightarrow $\sim 10^{20}$ target atoms/cm³ \longleftrightarrow $\gtrsim 1$ liter ACTIVE VOLUME

B2. Up Conversion of Zeeman Transition

- material transparent to the pump until an **AXION** is absorbed ($1 \rightarrow 2$)
- transition $1 \rightarrow 2$ takes place between **GS ZEEMAN-SPLIT LEVELS** to allow for tunability (B_0 field) in the interesting axion mass range
- level 3 is fluorescent \implies detection can be accomplished via **IR single photon detectors**
- dopant (rare-earth ion) concentration compatible with transition rate by axion absorption R_i for a **MOLE** of target atoms:

$$\begin{aligned}
 N_A R_i &= g_i^2 N_A \bar{v}^2 \frac{2\rho_a}{f_a^2} \min(t, t_1, t_a) \\
 &= \frac{2.13 \times 10^3}{\text{sec}} \left(\frac{\rho_a}{\text{GeV/cm}^3} \right) \left(\frac{10^{11} \text{ GeV}}{f_a} \right)^2 \\
 &\quad \cdot g_i^2 \left(\frac{\bar{v}^2}{10^{-6}} \right) \left(\frac{\min(t, t_1, t_a)}{\text{sec}} \right)
 \end{aligned}$$

P. Sikivie, PRL 113, 201301 (2014)



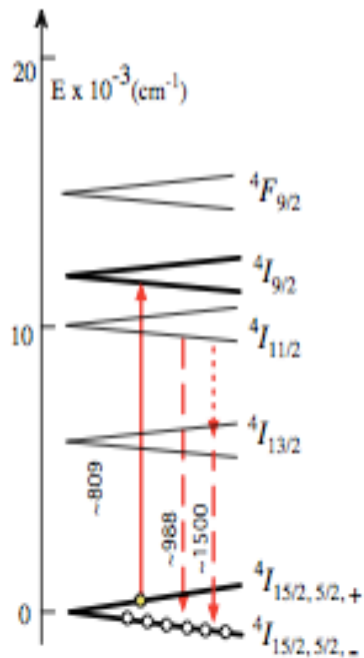
Doped Paramagnetic Optical Crystals

1% \longleftrightarrow $\sim 10^{20}$ target atoms/cm³ \longleftrightarrow $\gtrsim 1$ liter ACTIVE VOLUME

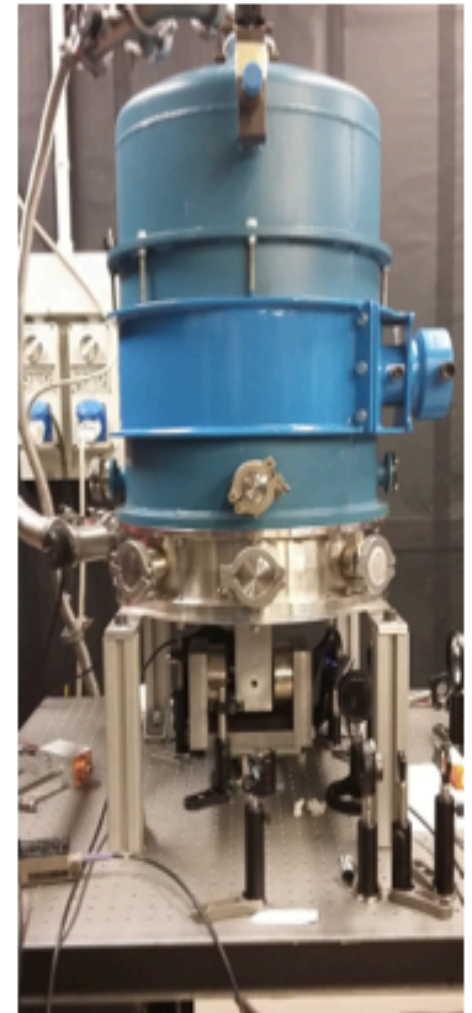
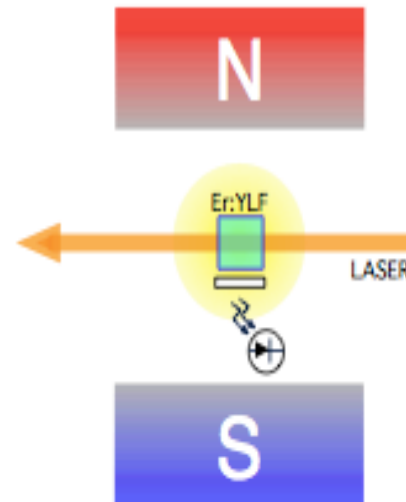
B4. First Measurements

Laser Induced IR Fluorescence

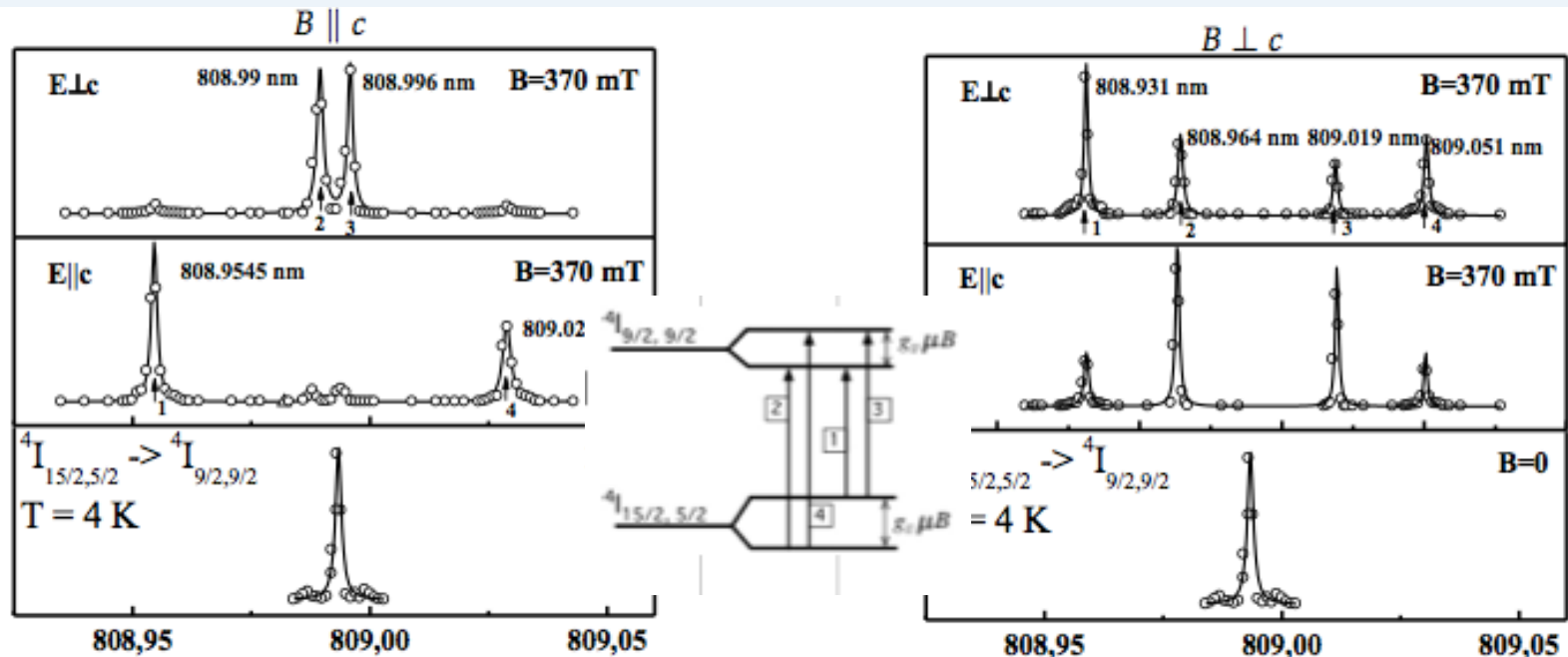
- Er:YLF (0.01%, 1% doping), oriented
- immersed in liquid He (4.2 K)/superfluid He (1.51 K)
⇒ axion transition saturated
- tunable laser (Ti:Sa)
- infrared (1.5 μm) fluorescence scheme
- $B_0 = 370 \text{ mT}$ (permanent magnet)



- ▶ identify Zeeman splitting
- ▶ investigate laser-induced noise (in a LIF scheme that involves phonon generation)



B5. Zeeman Up Converted Transitions



$$\lambda_3 - \lambda_1 = 41.3 \text{ pm} \rightarrow 78.2 \mu\text{eV} \rightarrow 18.9 \text{ GHz}$$

$$\lambda_4 - \lambda_3 = 32.99 \text{ pm} \rightarrow 62.5 \mu\text{eV} \rightarrow 15.2 \text{ GHz}$$

$$\lambda_3 - \lambda_1 = 88 \text{ pm} \rightarrow 166.7 \mu\text{eV} \rightarrow 40.3 \text{ GHz}$$

$$\lambda_4 - \lambda_3 = 32 \text{ pm} \rightarrow 60.5 \mu\text{eV} \rightarrow 14.7 \text{ GHz}$$

By comparison with data in the literature we are able to identify the splitting of the ground state in the (A) upconversion scheme with $B \parallel c$.

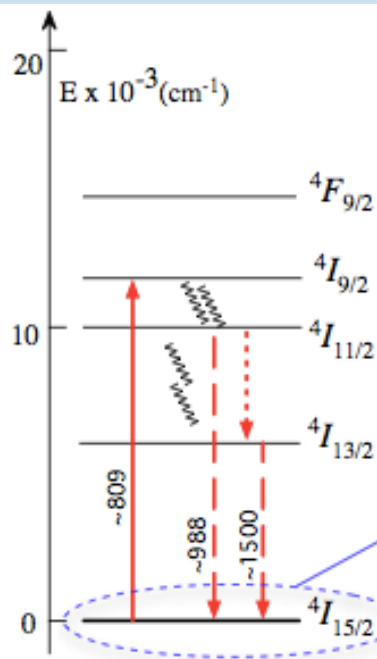
Navigation icons: back, forward, search, etc.

NO ATOMS IN THE EXCITED STATE REQUEST

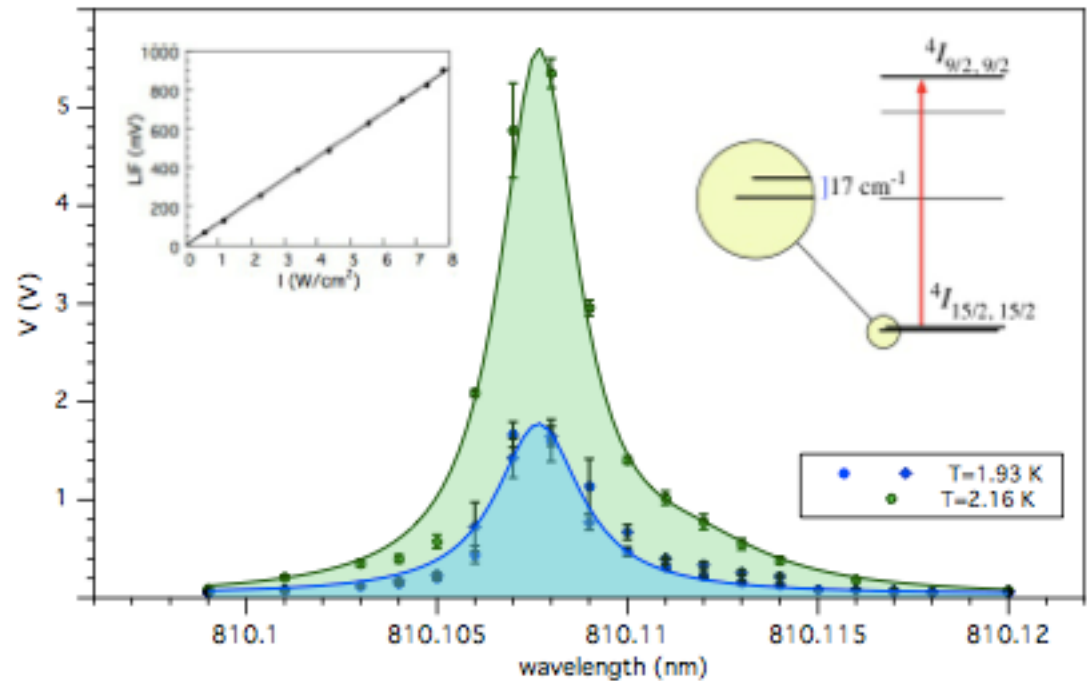
$$N_A e^{-(m_a/T)} < 0.1 \leftrightarrow T = 12 \text{ mK} \left[\frac{m_a(\text{eV})}{0.6 \cdot 10^{-4}} \right] = 15.6 \text{ mK} \implies \uparrow B_0 \text{ field (thus } m_a) \text{ to operate at } T \sim 200 \text{ mK}$$

B6. Laser Induced Background Study

Is the laser **heating** the crystal? / At which level is the **transparency condition** not satisfied? Measure the temperature of the active volume of the detector via LIF from the Stark levels.

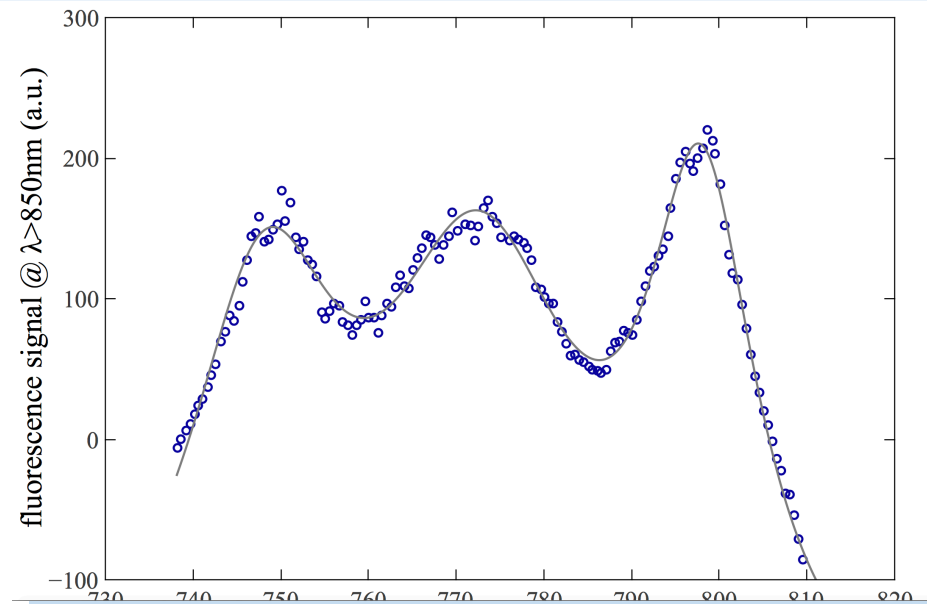
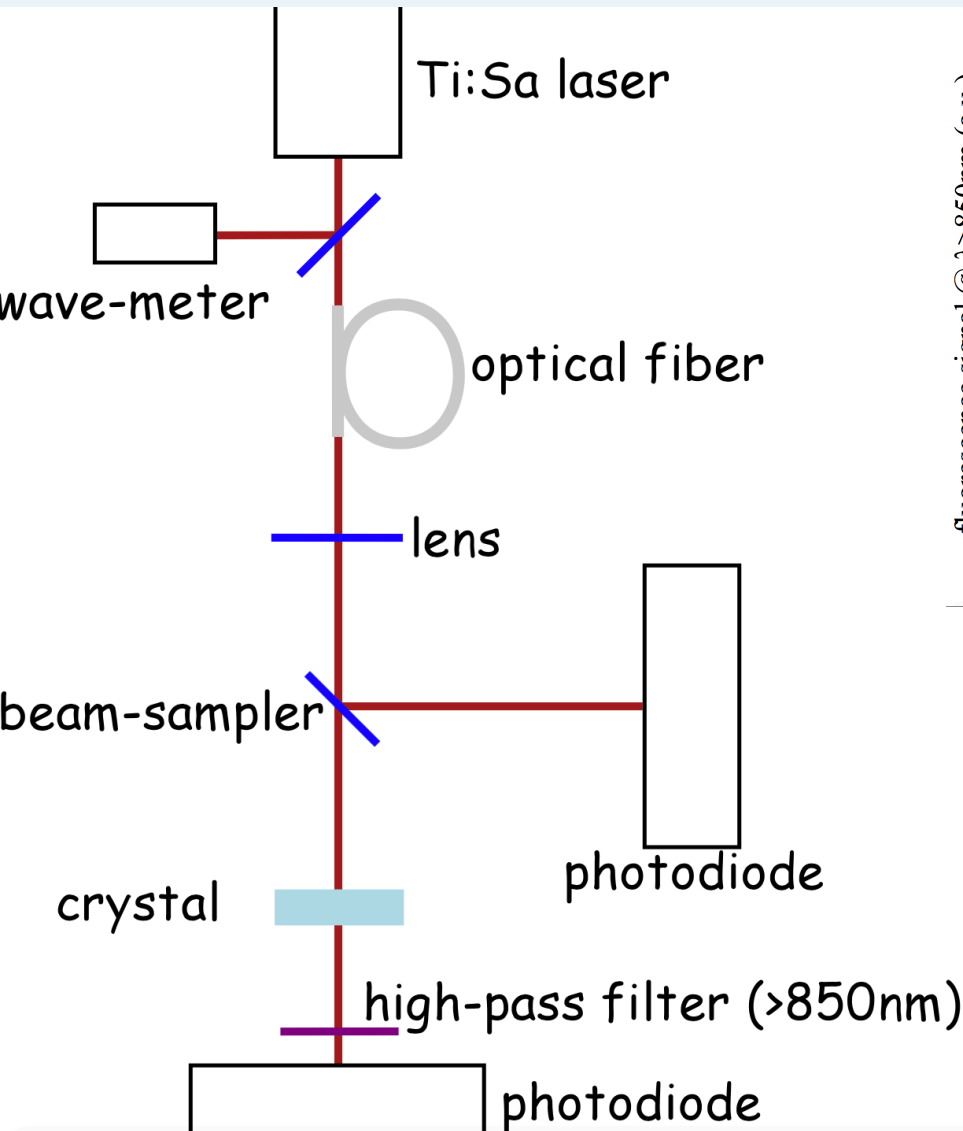


Stark split $^{2S-1}L_J$ level	$ M_J $	$E_{\text{exp}} (\text{cm}^{-1})$
$4I_{15/2}$	5/2	0
	15/2	17
	3/2	28
	1/2	57
	9/2	255
	7/2	290
	11/2	320
	13/2	355



No Measured Background at $T = 1.8$ Kelvin

4 kelvin Argon Crystal Rubidium doped @1%



Instead of 1 line 5 s-5 p

We observed 3 lines

To be understood

C) Inverse Bremsstrahlung electron acceleration under Laser Field combination of electron and light multiplication present in high density media

Electrons acceleration-multiplication in **high density materials**

- High dense gas (Ar, Xe, Kr)
- High power IR Laser light pump
- Charge signal
- Light emission signal

$$\sigma(\epsilon, \omega) = \frac{8\pi}{3} \frac{(v_i v_f)^2}{\omega^3} NQ(\epsilon) \frac{e^2}{\hbar c}$$

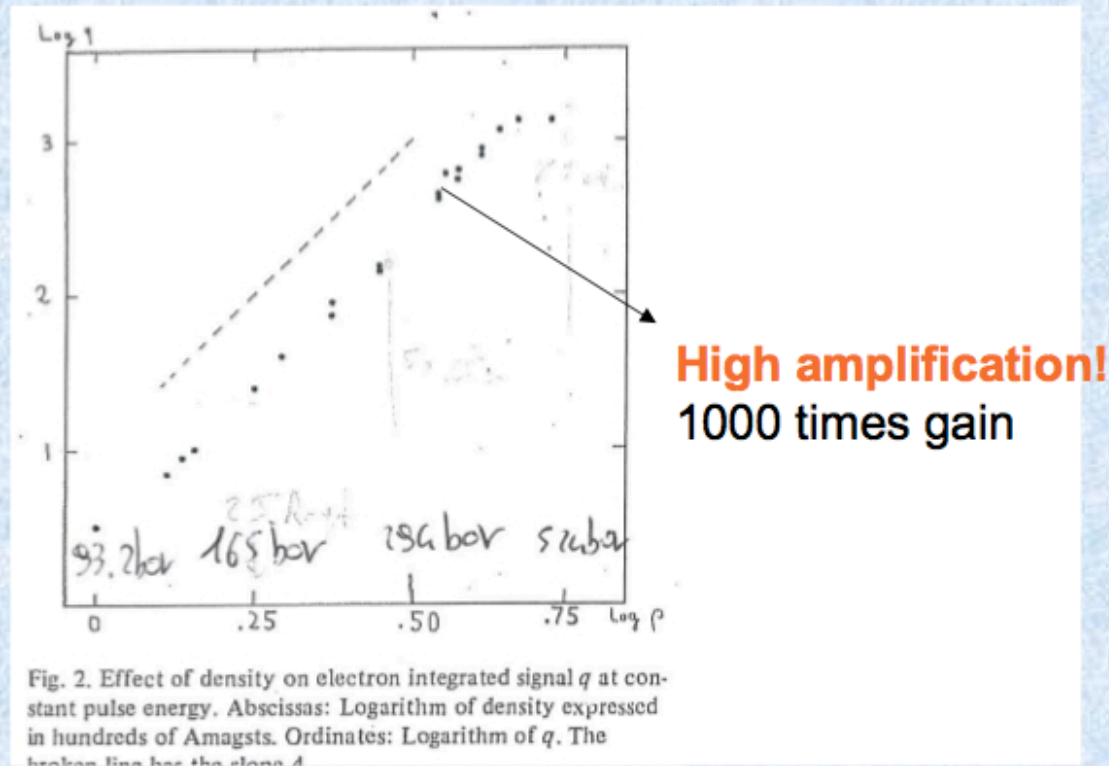


Fig. 2. Effect of density on electron integrated signal q at constant pulse energy. Abscissas: Logarithm of density expressed in hundreds of Amagsts. Ordinates: Logarithm of q . The broken line has the slope 4.

- † G. Hauchecorne, et al, *Photoionization experiments in dense argon gas*, Opt. Comm., 38, 3, (1981)
- G. Mayer, *Laser induced multiplication and visualization of free electrons in dense monoatomic gases*, Nucl. Instrum. Meth A, A254 (1987)

Operation of a ferromagnetic axion haloscope at $m_a = 58 \mu\text{eV}$

N. Crescini^{1,2,a} , D. Alesini³, C. Braggio^{1,4}, G. Carugno^{1,4}, D. Di Gioacchino³, C. S. Gallo², U. Gambardella⁵, C. Gatti³, G. Iannone⁵, G. Lamanna⁶, C. Ligi³, A. Lombardi², A. Ortolan², S. Pagano⁵, R. Pengo², G. Ruoso^{2,b} , C. C. Speake⁷, L. Taffarello⁴

¹ Dipartimento di Fisica e Astronomia, Via Marzolo 8, 35131 Padua, Italy

² Laboratori Nazionali di Legnaro, INFN, Viale dell'Università 2, 35020 Legnaro, Padua, Italy

³ Laboratori Nazionali di Frascati, INFN, Via Enrico Fermi, 40, 00044 Frascati, Rome, Italy

⁴ Sezione di Padova, INFN, Via Marzolo 8, 35131 Padua, Italy

⁵ Sezione di Napoli, INFN, University of Salerno, Via Giovanni Paolo II 132, 84084 Fisciano, Italy

⁶ Sezione di Pisa, INFN, University of Pisa, Largo Bruno Pontecorvo 3, 56127 Pisa, Italy

⁷ School of Physics and Astronomy, University of Birmingham, Birmingham, West Midlands B15 2TT, UK

Received: 1 June 2018 / Accepted: 19 August 2018

© The Author(s) 2018

Abstract Axions, originally proposed to solve the strong CP problem of quantum chromodynamics, emerge now as leading candidates of WISP dark matter. The rich phenomenology associated to the light and stable QCD axion can be described as an effective magnetic field that can be experimentally investigated. For the QUAX experiment, dark matter axions are searched by means of their resonant interactions with electronic spins in a magnetized sample.

matter fraction is 5.7%, meaning that DM is about five times more abundant than ordinary baryonic matter. This outstanding result triggered theoretical studies aiming to understand the nature of DM, for instance in the form of new particles beyond the Standard Model (SM).

The axion is a good candidate for DM but was not originally introduced to account for this specific issue. To solve the strong CP problem Peccei and Quinn added a new symme-

SCIENTIFIC REPORTS

OPEN

Axion dark matter detection by laser induced fluorescence in rare-earth doped materials

Caterina Braggio¹, Giovanni Carugno¹, Federico Chiossi¹, Alberto Di Lieto², Marco Guarise¹, Pasquale Maddaloni^{3,4}, Antonello Ortolan⁵, Giuseppe Ruoso ⁵, Luigi Santamaria⁶, Jordanka Tasseva⁴ & Mauro Tonelli²

We present a detection scheme to search for QCD axion dark matter, that is based on a direct interaction between axions and electrons explicitly predicted by DFSZ axion models. The local axion dark matter field shall drive transitions between Zeeman-split atomic levels separated by the axion rest mass energy $m_a c^2$. Axion-related excitations are then detected with an upconversion scheme involving a pump laser that converts the absorbed axion energy (\sim hundreds of μeV) to visible or infrared photons, where single photon detection is an established technique. The proposed scheme involves rare-earth ions doped into solid-state crystalline materials, and the optical transitions take place between energy levels of $4f^N$ electron configuration. Beyond discussing theoretical aspects and requirements to achieve a cosmologically relevant sensitivity, especially in terms of spectroscopic material properties, we experimentally investigate backgrounds due to the pump laser at temperatures in the range 1.9 – 4.2 K. Our results rule out excitation of the upper Zeeman component of the ground state by laser-related heating effects, and are of some help in optimizing activated material parameters to suppress the multiphonon-assisted Stokes fluorescence.

Received: 1 September 2017

Accepted: 25 October 2017

Published online: 09 November 2017

Experimental setup for the growth of solid crystals of inert gases for particle detection

M. Guarise,^{1,2,a} C. Braggio,³ R. Calabrese,^{1,4} G. Carugno,³ A. Dainelli,² A. Khanbekyan,^{1,4} E. Luppi,^{1,4} E. Mariotti,⁵ M. Poggi,² and L. Tomassetti^{4,6}

¹*Dipartimento di Fisica e Scienze della Terra, Via G. Saragat 1, 44122 Ferrara, Italy*

²*INFN Laboratori Nazionali Legnaro, Viale dell'Università 2, 35020 Padua, Legnaro, Italy*

³*Dipartimento di Fisica e Astronomia and INFN Sezione di Padova, Via F. Marzolo 8, I-35131 Padua, Italy*

⁴*INFN Sezione di Ferrara, Via G. Saragat 1, 44122 Ferrara, Italy*

⁵*Dipartimento di Scienze Fisiche, della Terra e dell'Ambiente and INFN Siena, Via Roma 56, 53100 Siena, Italy*

⁶*Dipartimento di Matematica e Informatica, Via G. Saragat 1, 44122 Ferrara, Italy*

(Received 5 September 2017; accepted 9 October 2017; published online 14 November 2017)

Low energy threshold detectors are necessary in many frontier fields of the experimental physics. In this work, we present a novel detection approach based on pure or doped matrices of inert gases solidified at cryogenic temperatures. The small energy release of the incident particle can be transferred directly (in pure crystals) or through a laser-driven ionization (in doped materials) to the electrons of the medium that are then converted into free electrons. The charge collection process of the electrons that consists in their drift within the crystal and their extraction through the solid–vacuum interface gives rise to an electric signal that we exploit for preliminary tests of charge collection and crystal quality. Such tests are carried out in different matrices of neon and methane using an UV-assisted apparatus for electron injection in crystals. *Published by AIP Publishing.* <https://doi.org/10.1063/1.5003296>

